Is the Atlantic Ocean driving the recent variability in South Asian dust?

Priyanka Banerjee[1], Sreedharan Krishnakumari Satheesh[1,2], Krishnaswamy Krishna Moorthy[2]

[1]Divecha Centre for Climate Change, Indian Institute of Science, Bangalore, India
[2]Centre for Atmospheric and Oceanic Sciences, Indian Institute of Science, Bangalore, India

Correspondence to: Priyanka Banerjee (pbanerjee.ocean@gmail.com)

Abstract

This study investigates the large-scale factors controlling interannual variability of dust aerosols over South Asia during 2001-2018. We use a parameter $DA_{\%}$, which refers to the frequency of days in a year when high dust activity is experienced over a region, as determined by combination of satellite aerosol optical depth and Angstrom exponent. While positive sea surface temperature (SST) anomaly in the central Pacific Ocean has been important in controlling $DA_{\%}$ over South Asia during 2001-2010; in recent years, the North Atlantic Ocean has assumed a dominant role. Specifically, high $DA_{\%}$ is associated with warming in the mid-latitude and cooling in the sub-tropical North Atlantic SSTs: the location of the two southern arms of the North Atlantic SST tripole pattern. This shift towards a dominant role of the North Atlantic SST in controlling $DA_{\%}$ over South Asia ~~is associated~~ coincides with a recent shift towards persistently positive phase of the North Atlantic Oscillation (NAO) and a resultant positive phase of the spring-time SST tripole pattern. Interestingly, there has also been a shift in the relation between the two southern arms of the SST tripole and NAO, which has resulted in weakening of the southwest monsoon circulation over the northern Indian Ocean and strengthening of the dust-carrying westerlies and northerlies in the lower and mid-troposphere. Simulations with an earth system model show that the positive phase of the North Atlantic SST tripole pattern is responsible for 10% increase in dust optical depth over South Asia during May-September; with increases as much as 30% during the month of June. This increase is mainly due to transport by the westerlies at 800 hPa pressure level, which on average increases dust concentration at this pressure level by 20% during May-September and up to 50% during June.

1 Introduction

South Asia is believed to be highly vulnerable to the long-term impacts of climate change (Stocker et al., 2013). One of the ways in which the impact of climate change is felt in this region is via aerosol feedback on the regional climate (e.g., Satheesh and Ramanathan, 2000; Ramanathan et al., 2005; Bollasina et al., 2011). Mineral dust is the most important aerosol component (by mass) present in this region (e.g., Ginoux et al., 2012; Jin et al., 2018a; Banerjee et al., 2019). Several studies during the last two decades have shown that mineral dust can influence different aspects of the climate of South Asia with the largest focus given to dust impact on radiative balance (e.g., Deepshikha et al., 2006; Zhu et al., 2007; Pandithurai et al., 2008) and the southwest monsoon (SWM) precipitation (Vinoj et al., 2014; Jin et al., 2014; Solmon et al., 2015). However, to better appreciate dust-climate feedback, it is important to understand what large-scale factors control dust emission

and transport in this region and, if there are long-term changes in these controlling factors. At present, there is very little understanding of these factors, sometimes with lack of consensus among the studies.

There are some recent indirect evidences of El Niño /La Niña influencing dust fluxes over South Asia. For example, Kim et al. (2016) have reported that La Niña conditions are associated with increased absorbing aerosols over northwest India which, in turn, leads to positive feedback on the SWM precipitation. On the contrary, Abish and Mohankumar (2013) argued that increased zonal transport and subsidence over India during El Niño years can lead to enhanced absorbing aerosols like dust over India. A few other studies have shown that over Southwest Asia, variability of dust aerosols is controlled by climatic factors like El Niño /La Niña at interannual timescale (Notaro et al., 2015; Yu et al., 2015; Banerjee and Prasanna Kumar, 2016) and by Pacific Decadal Oscillation (PDO) at interdecadal timescale (Notaro et al., 2015; Yu et al., 2015; Pu and Ginoux, 2016). Eastward transport of dust from Southwest Asia by the mid-level westerlies are shown to contribute about 50% to the total dust optical depth over the Indo-Gangetic plain of South Asia (Banerjee et al., 2019) and can influence dust trend over this region. The Indian Ocean Dipole (IOD) is the other teleconnection that influences atmospheric circulation over this region, with the positive phase of IODs counteracting the impact of El Niño on precipitation over South and Southwest Asia (Ashok et al., 2001; 2004). This can reduce the magnitude of anomalies of dust over Southwest Asia due to an El Niño event (Banerjee and Prasanna Kumar, 2016). During the beginning of the 21st century, a positive trend in SWM precipitation due to the negative phase of Interdecadal Pacific Oscillation (Huang et al., 2020) has resulted in a negative trend of dust aerosol over South Asia (Pandey et al., 2017; Jin and Wang, 2018b). Ice core records in the central Himalayas have shown an inverse relation between the SWM precipitation and dust deposition (Thompson et al., 2000). During winter season, aerosol optical depth over northern India is shown to be positively correlated to simultaneous central Pacific Nino index and negatively correlated to Antarctic Oscillation during the preceding autumn (Gao et al., 2019).

The main dust source regions over South Asia are spread across the Thar Desert and the Indo-Gangetic plain in India and Pakistan; the Makran coast and the Hamun-I-Mashkel in Pakistan; the Margo Desert and the Rigestan Desert in Afghanistan (Walker et al., 2009; Ginoux et al., 2012). The Margo Desert, the Rigestan Desert and the Hamun-I-Mashkel receive predominantly winter precipitation from the Mediterranean low-pressure systems travelling eastwards. Rest of the regions receive summer precipitation from the SWM system, although the total amount of precipitation received is very low. It has been shown by several studies that one of the major factors controlling the interannual variability of the SWM rainfall is El Niño /La Niña with developing El Niño conditions over the Pacific Ocean leading to weakening of the SWM moisture influx (e.g., Sikka, 1980; Rasmusson and Carpenter, 1983; Ashok et al., 2004). Tropical Pacific Ocean warming (cooling) in El Niño region is also responsible for wetter (drier) than normal conditions over the winter precipitation region in Southwest Asia (Barlow et al., 2002; Mariotti, 2002). This implies that the conditions prevailing over the Pacific Ocean has an important role in controlling the level of dust activity over the northern Indian Ocean (IO) and South Asia either directly through precipitation impact on dust emission and/or indirectly through dust transport from Southwest Asia. However, in the backdrop of global warming and the internal variability of the Pacific Ocean at different timescales (e.g., Kosaka and Xie, 2016; Deser et al., 2017a), the well-known El Niño - monsoon relation has undergone changes in the recent decades. Since the late 1970s, the relation between El

Niño and negative rainfall anomaly over India has become less significant, possibly, due to the higher rate of warming of the Eurasian landmass in the recent years compared to the IO or due to the cooling of the Pacific Ocean (Kumar et al., 1999; Kinter et al., 2002). Simultaneously, the Atlantic Ocean has assumed a stronger role in modulating the monsoon circulation over the northern IO (Chang et al., 2001; Kucharski et al., 2007; Kucharski et al., 2008). While some studies have shown the importance of the sea surface temperature (SST) along the south equatorial Atlantic (Kucharski et al., 2007; Kucharski et al., 2008), other studies have shown that positive SST anomalies over the western North Atlantic centered on 40^{o}N latitude can lead to positive anomalies of monsoon over India (Srivastava et al., 2002; Rajeevan and Sridhar, 2008). Over the North Atlantic Ocean, the dominant mode of sea level pressure variability during winter is the North Atlantic Oscillation (NAO) (Hurrell, 1995). The tripole pattern of SST over the North Atlantic associated with the winter NAO (see e.g., Visbeck et al., 1998) can persist during spring and impact the summer circulation over Eurasia (Gastineau and Frankignoul, 2015; Osso et al., 2018). During summer months, two dominant modes of variability are the summer NAO (Folland et al., 2009) and the Summer East Atlantic (SEA) pattern (Osso et al., 2018; Osso et al., 2020). During the period 1948-2016, for the summer months of June-September, NAO explained about 36% of variance, while SEA explained about 16% of variance of sea level pressure (Osborne et al., 2020). A few studies have shown that such variability of SST and circulation over the North Atlantic has the potential to influence the SWM circulations over South Asia. For example, the SST anomalies associated with the Atlantic Multidecadal Oscillations can influence the tropospheric temperature leading to strengthening or weakening of the monsoon via modulation of the frequency and strength of NAO (Goswami et al., 2006). The cold (positive) phases of the SST tripole over the North Atlantic have induced stronger westerlies over the northern IO (Krishnamurthy and Krishnamurthy, 2015). The influences of the extra-tropical North Atlantic/Pacific SST on the South Asian monsoon are stronger during weak El Niño /La Niña years (Chattopadhyay et al., 2015).

In the above backdrop, we examine how changes in the spatial pattern of ocean warming during 2001-2018 have led to increased dependence of South Asian dust on the North Atlantic Ocean, shifting from the previously dominant influence of the equatorial Pacific SST. Using observations and reanalysis data we explore the physical mechanism by which a remote response of the circulation over South Asia is invoked by SST anomalies over the North Atlantic. We have further performed control and sensitivity studies using an earth system model to investigate in detail how dust emission and transport is impacted by perturbing SST over the North Atlantic Ocean. For this study, we have chosen a domain encompassing 65^{o}E-82^{o}E longitude and 24^{o}N-32^{o}N latitude. We consider this as the dust belt of South Asia. The region is influenced predominantly by SWM precipitation. Unless stated otherwise, all analyses involving spatial averaging focus only on this region.

2 Data and Models

2.1 Satellite observation and reanalysis data

The main source of dust aerosol data for this study is from the Moderate Resolution Imaging Spectroradiometer (MODIS) aboard Terra (2001-2018) and Aqua (2003-2018) satellites, which provide the longest satellite-based information on both aerosol load and size distribution over land and ocean. We have calculated frequency of days in a year when substantial dust activity is experienced over South Asia (DA$_{\%}$) using MODIS level 3 version 6.1 daily deep blue aerosol optical depth (τ) and Angstrom exponent (α). The deep blue algorithm of

MODIS is used to retrieve aerosol information over bright surfaces, like arid regions, where surface reflectance is low at the blue end of the spectrum (Hsu et al., 2004; Hsu et al., 2006). The criteria used for estimating $DA_{\%}$ are (i) $\tau > 0.6$ and (ii) $\alpha < 0.2$ to isolate the days dominated by moderately high load of coarse-mode aerosols. This yields a map of the main dust source regions in and around South Asia at $1^{o}X1^{o}$ horizontal resolution. Previously, along with deep blue τ and α, single scattering albedo has also been used to account for the absorptive property of dust when deriving dust optical depth (Ginoux et al., 2012; Pu and Ginoux, 2018). For our present purpose, τ and α combination is sufficient since we are deriving frequency of days of dust activity and not the absolute optical depth. Fig. 1a shows the spatial distribution of $DA_{\%}$ averaged for 2001-2018 and its standard deviation (SD). High values of $DA_{\%}$ coincide with known locations of dust source regions. The SD is high indicating that these dust source regions experience significant interannual variability of $DA_{\%}$. The inset in Fig. 1a shows the monthly climatology of $DA_{\%}$ with the SD, which reveals that highest values occur during June-July and lowest values during November. Over the dust belt of South Asia, for 2001-2018, average $DA_{\%}$ from MODIS Terra is 5.2 (SD is 1.7) and from MODIS Aqua is 4.2 (SD is 1.7). Changing the threshold values of both τ and α by 50% and recalculation of $DA_{\%}$ does not lead to any significant changes in these results. MODIS-derived $DA_{\%}$ matches well with year-to-year variability of dust optical depth (τ_d) from Infrared Atmospheric Sounder Interferometer (IASI) aboard Metop-A (2008-2018) with a correlation coefficient of 0.73, which is significant at 99% confidence level (Fig. 1b). IASI reports τ_d at 10 μm wavelength and at a spatial resolution of $0.5^{o}X0.5^{o}$ (Capelle et al., 2018). For 2008-2018, IASI dataset yields annual average τ_d value of 0.17 (SD of 0.02). In subsequent analysis, we use combined $DA_{\%}$ obtained from MODIS Terra and Aqua.

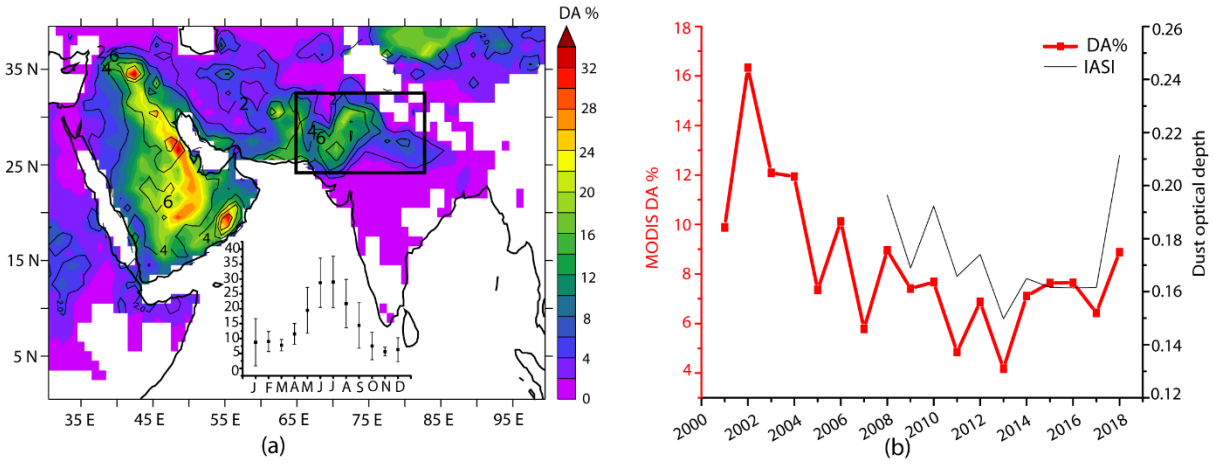

Figure 1: (a) Shading shows spatial distribution of $DA_{\%}$ averaged for 2001-2018 and contours are the standard deviations of $DA_{\%}$ for the same period. The black rectangle indicates the dust belt of South Asia (65°E-82°E, 24°N-32°N) which is used for subsequent analysis. The monthly climatology and the standard deviation of $DA_{\%}$ over dust belt of South Asia are shown by black squares and vertical bars respectively in the inset. (b) Time-series of MODIS-derived $DA_{\%}$ and IASI-retrieved annual dust optical depth over the dust belt of South Asia.

To examine the linkages between the spatial variability of SST during different periods and South Asian dust activity, we have used 3 SST datasets: (1) National Oceanic and Atmospheric Administration (NOAA) Extended Reconstructed SST (ERSST) version 5 (Huang et al., 2017) available at $2^{o}X2^{o}$ spatial resolution, (2)

Centennial in situ Observation-Based Estimates (COBE) version 2 SST data at 1°X1° spatial resolution (Hirahara et al., 2014) and (3) Optimally Interpolated SST version 2 (OISST) data at 1°X1° spatial resolution (Reynolds et al., 2002). All the SST datasets are at monthly temporal resolution. The ERSST version 5 data combines ship and buoy SST from International Comprehensive Ocean and Atmosphere Dataset (ICOADS) along with Argo data since 2000. COBE also uses ICOADS data along with data from Kobe collection. Finally, OISST combines Advanced Very High Resolution Radiometer (AVHRR) retrievals with ship-borne and buoy data. To separate the impact of the Atlantic Ocean on dust from the Pacific, partial correlations between SST and $DA_{\%}$ have been calculated using the following relation:

$$r_{12,3} = \frac{r_{12} - r_{13}r_{23}}{\sqrt{(1-r_{13}^2)(1-r_{23}^2)}} \quad (1)$$

where, $r_{12,3}$ is the correlation between variables 1 and 2 after removing the impact of variable 3. In equation (1), r_{ij} refers to correlation between variables i and j.

Atmospheric data such as wind vectors, geopotential height, sea level pressure and velocity potential have been taken from National Centers for Environmental Prediction/ National Center for Atmospheric Research (NCEP/NCAR) Reanalysis at 2.5°X2.5° spatial resolution (Kalnay et al., 1996). For precipitation we have used monthly Global Precipitation Climatology Project (GPCP) version 2.3 data available at 2.5°X2.5° spatial resolution, which combines rain gauge measurements with satellite observations (Huffman et al., 1997). Additionally, monthly precipitation data averaged from daily data has been obtained from Precipitation Estimation from Remotely Sensed Information using Artificial Neural Networks (PERSIANN) at 0.25°X0.25° spatial resolution. PERSIANN algorithm is applied on Gridded Satellite (GridSat-B1) brightness temperature observation in the infrared region (Ashouri et al., 2015). The precipitation data are then corrected for bias against GPCP precipitation estimates. To track the large-scale variability over North Atlantic, Hurrell's station-based seasonal NAO index has been used for the years 2001-2018 (Hurrell, 1995; Hurrell and Deser, 2009). NAO index is calculated based on the difference between normalized sea level pressure over Lisbon, Portugal and Stykkisholmur/Reykjavik, Iceland.

2.2 CESM experiments

Simulations were carried out using the Community Earth System Model (CESM) version 1.2 to examine the mechanism by which SST anomalies over the North Atlantic Ocean impact dust cycle over South Asia. CESM is a fully coupled model used for simulations of global climate across different spatial and temporal scales. There are several components to CESM model (example atmosphere, land, sea ice, ocean etc.), which are linked through a coupler. We have used Community Atmosphere Model version 4 with the Bulk Aerosol Module (CAM4-BAM) coupled with Community Land Model version 4 in "Satellite Phenology" (CLM-SP) configuration. Simulations are carried out for trace gases levels corresponding to the year 2000 at 0.9°X1.25° spatial resolution with 26 levels in the vertical.

Emission of dust is calculated within CLM model, while dust transport and deposition, as well as the radiative effects are calculated within CAM model (Mahowald et al., 2006). Dust emission follows the treatment of Dust Entrainment and Deposition scheme of Zender et al. (2003a). Dust emission is based on saltation process, which

depends on modelled wind friction velocity, soil moisture, vegetation, and snow cover. This saltation flux occurs whenever wind friction velocity exceeds a threshold (Marticorena and Bergametti, 1995). Additionally, dust emission is corrected by a geomorphic source function, which accounts for the spatial variability of erodible materials (Zender et al., 2003b). In CAM4-BAM dust is emitted in 4 size bins: 0.1-1.0, 1.0-2.5, 2.5-5.0 and 5.0-10.0 μm. Dust is transported based on CAM4 tracer advection scheme and is removed via dry (gravitational and turbulent deposition) and wet depositions (convective and large-scale precipitation) (Zender et al., 2003a; Neale et al., 2010). The solubility factor and scavenging coefficient are taken here as 0.15 and 0.10, respectively.

Two sets of simulations have been carried out with CESM: (1) the "Ctrl" simulation, where the atmosphere was forced with prescribed climatological monthly SST and sea ice from Hadley Centre (1870-1981) (Rayner et al., 2003) and NOAA Optimal Interpolation SST (1981-2010) (Hurrell et al., 2008), and (2) the "NAtl" simulation, where the month-by-month observed trend in SST during 2011-2018 were imposed over the climatological SST only over the North Atlantic Ocean, that is, over the region 5ºN-80ºN latitude and 5ºW-85ºW longitude. Over rest of the domain climatological SST from Hurrell was prescribed. Thus, the differences between "NAtl" and "Ctrl" simulations reflect solely the impact of North Atlantic SST anomalies, as observed during 2011-2018, on atmospheric circulation and dust load. A total of 15 years of simulations have been carried out for each of Ctrl and NAtl cases with each year being initialized from the atmospheric state at the end of the previous year. For this study, monthly mean values for the last 10 years of model runs have been used for both the cases. In the following section we have assessed CESM simulations of atmospheric circulation and dust over the study region.

2.3 Model validation

In general, CESM simulations can reproduce the main features of the North Atlantic summer climate and circulation, on which we are focussed here. Sea level pressure-based empirical orthogonal analysis carried out for CESM Large Ensemble simulations for 1920-2012 have revealed that NAO accounts for 40-member mean variance of 43% for winter months (Deser et al., 2017b). With our ten years CESM simulation we can still identify the dominant modes of variability. Empirical orthogonal function using June-September sea level pressure from CESM shows that NAO accounts for 63% and SEA pattern accounts for 14% of sea level pressure variances (Supplementary Fig. S1). To examine CESM performance over South Asia we have compared outputs from CESM Ctrl simulation with NCEP/NCAR wind at 850 hPa pressure level and PERSIANN precipitation separately for the spring inter-monsoon (April-May) and SWM (June-September) periods in Figs. 2 a-d. The comparisons reveal that the Ctrl run reproduces the main features of circulations and precipitation over South Asia quite well, although with certain biases, which impact dust distribution and its temporal evolution. During April-May anomalous westerlies drive positive precipitation bias over peninsular India and southeast Bay of Bengal (Figs. 2 a and b). The anomalous southerlies over the southern part of the Indo-Gangetic plain lead to negative precipitation bias there, but a positive bias over the eastern Himalayas. During June-September, there are positive biases of precipitation along the west coast of India, southern India, the Himalayan foothills and most of the Middle East. Negative bias in precipitation prevails over eastern India and Southeast Asia bordering northeastern Bay of Bengal (Figs. 2 c and d). The positive bias along the west coast of India is associated with stronger westerlies in the Ctrl run. The anomalous anticyclone over the northern

Bay of Bengal leads to negative bias in precipitation of around 30%. This dipole in precipitation bias over the South Asian monsoon region has been recognized in Coupled Model Intercomparison Project Phase 5 (CMIP5) suite of models (Sperber et al., 2013) and has been attributed to several causes: SST bias over western equatorial IO (Annamalai et al., 2017); suppression of moist convection processes due to smoothening of topography (Boos and Hurley, 2013); weak advection of cold-dry air off Somali coast which reduces available moisture (Hanf and Annamalai, 2020). Comparing temporal evolution of CESM simulated precipitation with observations from PERSIANN (Figs. 2 e and f) we see that generally wet bias prevails over both Indian domain (Fig. 2e) and the South Asian dust belt (Fig. 2f). CESM simulates one-month delay in the peak monsoon rainfall over these regions.

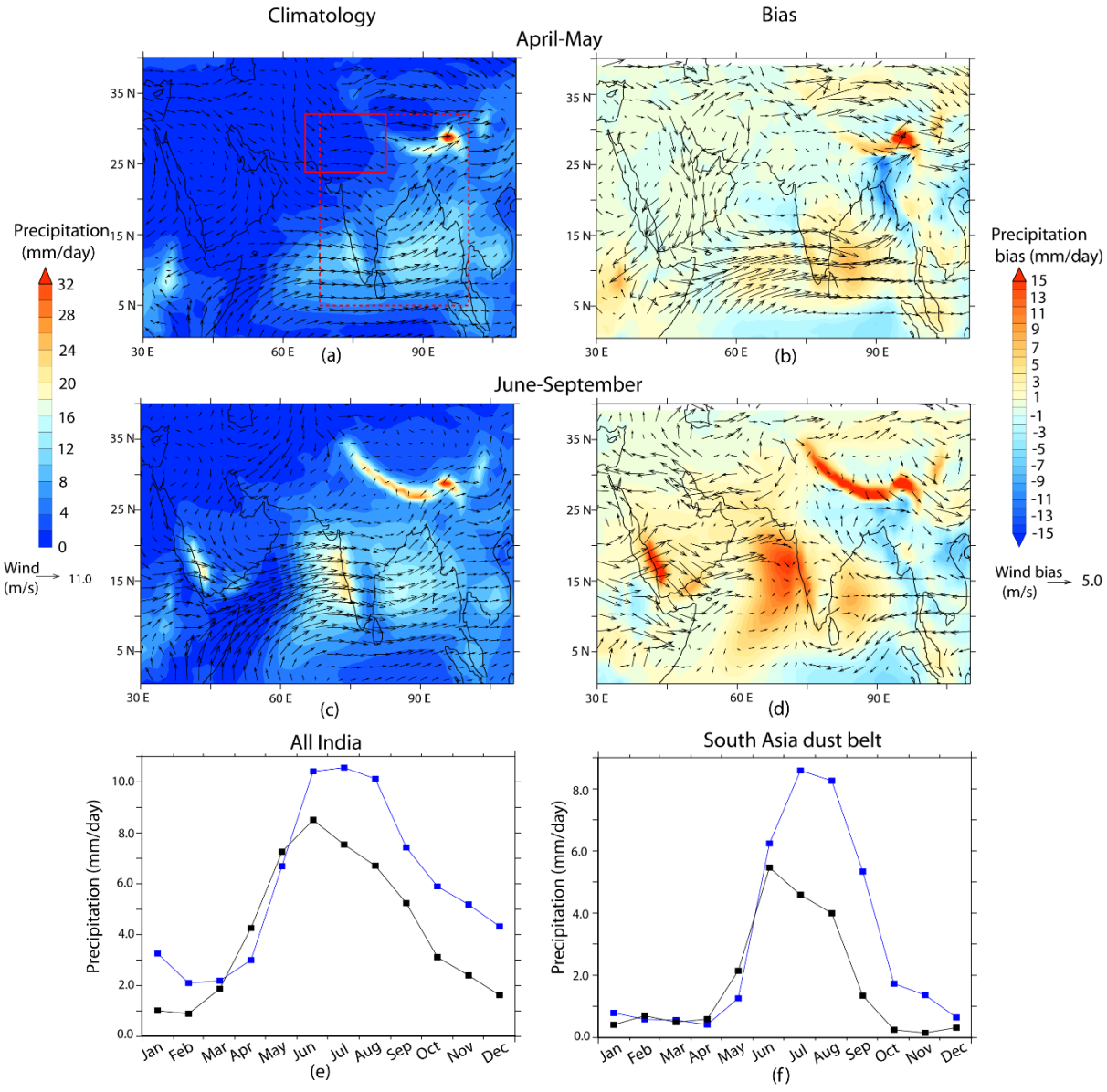

Figure 2: Comparison of CESM-Ctrl simulation with observations/reanalysis data. CESM simulated climatology of precipitation and wind for (a) April-May and (c) June-September are shown. Differences between CESM simulated precipitation (shading) with that of PERSIANN and CESM simulated wind (arrows) with that of NCEP/NCAR reanalysis at 850 hPa pressure level are given for (b) April-May and (d) June-September. Time evolution of CESM (blue curve) and PERSIANN precipitation (black curve) over (e) All India (5ºN-32ºN latitude, 68ºE-100ºE longitude)

and (f) the South Asian dust belt (24ºN-32ºN latitude, 65ºE-82ºE longitude). These domains are, respectively, indicated in (a) by dashed and continuous red boxes.

With respect to CESM simulation of dust, we have compared dust optical depth (τ_d) from Ctrl run with IASI-retrieved τ_d and coarse mode τ data from Aerosol Robotic Network (AERONET) stations at Kanpur (2001-2018), Lahore (2010-2016) and Jaipur (2010-2017). For this, we have used version 3 AERONET level 2.0 cloud cleared aerosol data. In general, CESM Ctrl reproduces the main dust emission regions over South and Southwest Asia (Fig.3a) along with temporal evolution of τ_d (Fig.3b). However, the positive bias in precipitation over dust source region, prevailing almost throughout the year, leads to underestimations of τ_d compared to observations. This discrepancy between CESM and observations is low during the winter months and increases during the monsoon months when CESM simulates about 3.5 mm day^{-1} positive bias in precipitation over the South Asian dust belt and ~2 m s^{-1} easterly wind bias. For example, during May when τ_d peaks, CESM simulates τ_d of ~0.2, while AERONET coarse mode τ over Kanpur, Jaipur and Lahore are almost double. Negative bias in CESM τ_d is also apparent when compared to IASI-observed 10 µm τ_d over South Asia (Fig.3b). Although precipitation bias during April-May is low (~0.1 mm day $^{-1}$, Fig. 2b), easterly wind bias of 0.7 m s^{-1} leads to low transport from the west. Similar negative bias in dust associated with weak northwesterlies over the Indo-Gangetic plain has been noted for CESM-CAM5 simulation submitted to CMIP5 (Sanap et al., 2014). One important reason for CESM underestimation of τ_d can be the exclusion of anthropogenic sources of dust, which contributes to nearly half of the total annual dust emission (Ginoux et al., 2012). Several improvements in simulating dust with CESM have been suggested by updating dust emission size distribution, optical properties, wet deposition parameterizations and tuning soil erodibility (Albani et al., 2014). While further improvements in CESM for better representation of dust cycle over South Asia is a topic for future, in case of this study, notwithstanding the negative bias, CESM Ctrl simulation is able to simulate the pattern of spatial distribution and seasonal evolution of South Asian dust. This is adequate for the present work as we are here interested in the direction of change in simulated dust load due to the North Atlantic SST tripole rather than on the absolute magnitude of τ_d.

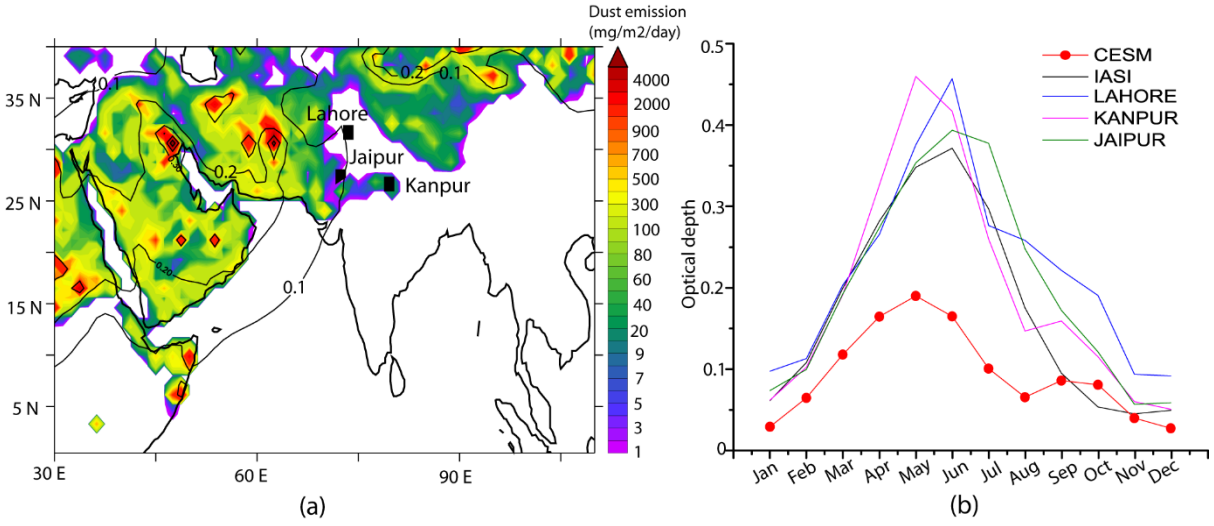

Figure 3: (a) Shading shows the distribution of main dust emitting regions from CESM and the contours indicate dust optical depth. Both parameters have been averaged for ten model years. (b) Comparison of monthly climatology

of dust optical depth over the South Asian dust belt from CESM-Ctrl simulation with IASI and AERONET (Lahore, Kanpur, and Jaipur) observations.

3 Results and discussion

We first demonstrate that there is a change in the relation between dust aerosol variability over South Asia and global SSTs during 2001-2018 with the role of the North Atlantic Ocean assuming importance in the recent years. We next discuss the possible physical mechanism involved by which SST anomalies over key regions in the North Atlantic influence the circulation over South Asia. Finally, CESM simulation results are used to isolate the effect of North Atlantic SST variability on dust emission and transport over South Asia.

3.1 Decadal change in correlation between dust and SST

We have carried out correlation analysis of $DA_{\%}$ over the dust belt of South Asia with annual averaged SSTs separately for the periods 2001-2010 and 2011-2018. ~~These are the two periods when the signature of shift from the Pacific to the Atlantic SST modulation of $DA_{\%}$ is the strongest.~~ The maps showing spatial distribution of the correlation coefficients for these two periods are shown, respectively, in Figs. 4 a-b ~~Figures 4a and b~~. During 2001-2010, the largest coherent region with which $DA_{\%}$ shows significant positive correlation encompasses central equatorial Pacific (Fig. 4a; marked by continuous rectangle). During 2011-2018 this region has contracted and shifted north-westwards (Fig. 4b; continuous rectangle), while two new regions of significant correlations have emerged: (1) over mid-latitude North Atlantic centered on 40°N latitude (significant positive correlation) and (2) over sub-tropical North Atlantic centered on 20°N latitude off the western coast of North Africa (significant negative correlation). These two regions are shown by dashed rectangles and are marked as "1" and "2" respectively in Fig. 4b. Though a weak signature of this correlation pattern is present in 2001-2010, it has emerged significantly strong during 2011-2018. Conducting month-by-month analysis of the impact of SST on $DA_{\%}$ (not shown) it is seen that the positive correlation between $DA_{\%}$ and SST over central equatorial Pacific during 2001-2010 is most prominent during September-October; while that over the North Atlantic during 2011-2018 is most prominent during April-June, which are used here for subsequent analysis. We have constructed a North Atlantic Difference Index (NADI) of SST by taking into account the regions where $DA_{\%}$ have significant correlation with the North Atlantic SST as seen in Fig. 4b. NADI is the standardised difference in SST over mid-latitude (Region 1, taken as 70°W-25°W longitude, 25°N-40°N latitude) and sub-tropical (Region 2, taken as 70°W-25°W longitude, 10°N-20°N latitude) North Atlantic, averaged for April-June. Furthermore, Fig. 4c shows 8-year running correlations between $DA_{\%}$ over South Asia and central equatorial Pacific SST (taken as 175°W-140°W longitude, 5°N-5°S latitude) and April-June NADI, which clearly demonstrates the transition from Pacific control of dust during 2001-2010 to North Atlantic control of dust during 2011-2018. This justifies our basis of separation of the two periods in Figs. 4 a-b. Fig. 4d~~e~~ depicts the variation of correlation coefficient between April-June NADI and monthly $DA_{\%}$ over South Asia separately for 2001-2010 and 2011-2018. Monthly $DA_{\%}$ is simply the percentage of days in a month when $\tau > 0.6$ and $\alpha < 0.2$. Fig. 4~~c~~d clearly shows that the correlation between NADI and $DA_{\%}$ is stronger and significant (at 95% confidence level) for 2011-2018, during May-October, in comparison to 2001-2010. These months having significant correlation largely coincide with the high dust months over South Asia, where dust loads peak during

May-June. During 2001-2010, partial correlation between annual NADI and annual $DA_{\%}$ adjusted for annual central equatorial Pacific SST is 0.19. During 2011-2018, this improves to 0.82, which is significant at 99% confidence level. For 2001-2010, a significant negative relation between NADI and $DA_{\%}$ is seen only for the month of February.

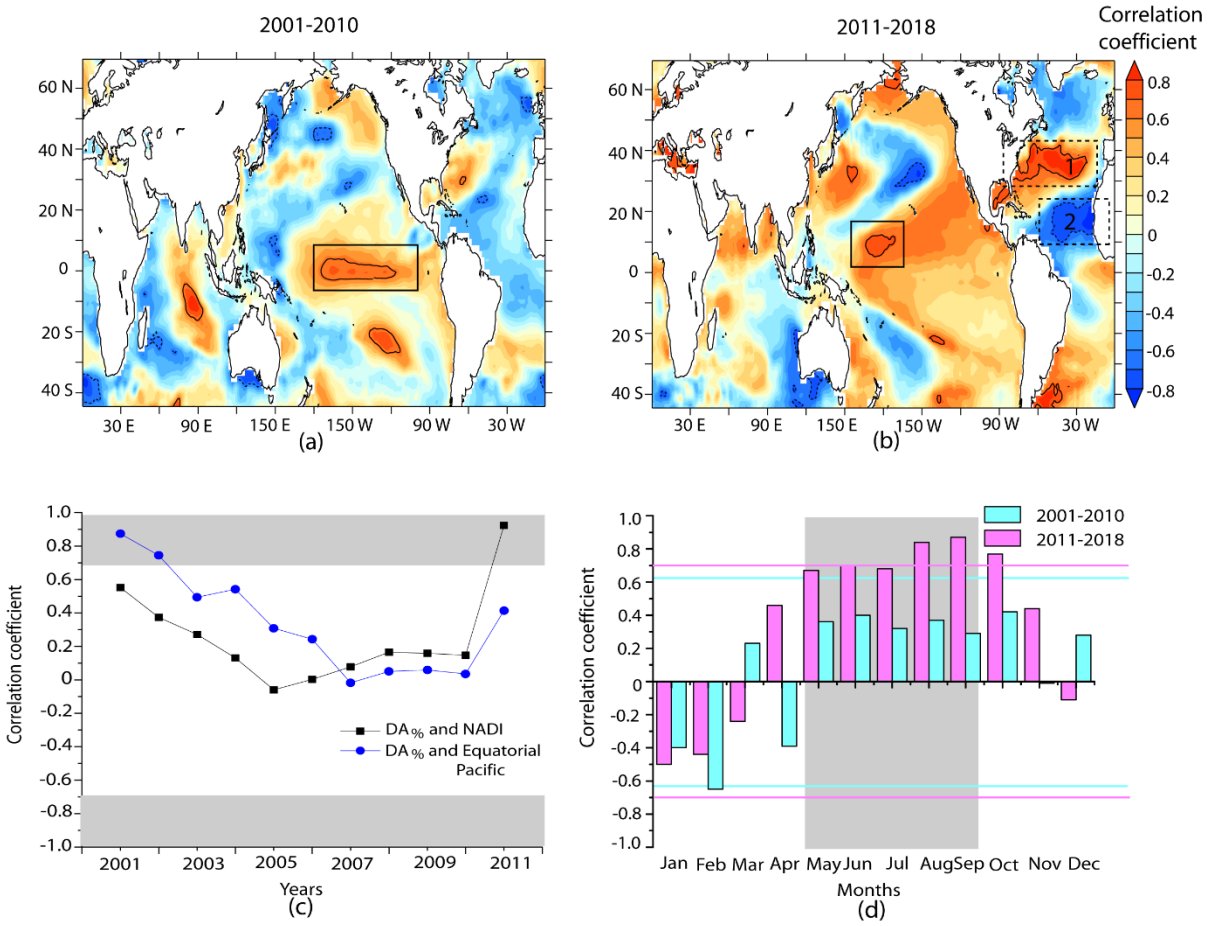

Figure 4: Correlation between percentage frequency of annual dust activity ($DA_{\%}$) and annual average SST for (a) 2001-2010 and (b) 2011-2018. The black contours enclose the regions where correlation coefficient is significant at 95% confidence level. The continuous (dashed) boxes show the main regions with which $DA_{\%}$ over South Asia have significant correlations over the Pacific (Atlantic) Ocean (see text for details). In (b) the regions used for constructing the North Atlantic Difference Index (NADI) are marked as "1" and "2". (c) 8-year running correlation between $DA_{\%}$ and April-June NADI (black curve) and $DA_{\%}$ and the September-October central equatorial Pacific SST (blue curve). Horizontal axis shows the first year for each correlation window and the grey shaded regions mark the locations of 95% significant level. (~~c~~d) Correlation between April-June NADI and monthly $DA_{\%}$ are plotted. The blue and pink horizontal lines indicate the 95% confidence levels for 2001-2010 and 2011-2018 respectively. The grey shaded region highlights the months which have $DA_{\%}$ values greater than annual average $DA_{\%}$.

The central equatorial Pacific, where the SST is significantly correlated with $DA_{\%}$ during 2001-2010, is historically a prime region driving the variability of the SWM, and by some extension, dust emission and transport. Since the 1990s, stronger El Niño signals have been detected in the central Pacific SST compared to the eastern Pacific (Yeh et al., 2009; Lee and McPhaden, 2010). Interestingly, there has been a cooling trend in

the central Pacific SST during 2001-2010 (of -0.8°C decade^{-1}) when this region was a major driver of $DA_{\%}$ over South Asia (continuous box in Fig.5a). This formed a part of the hiatus within the ongoing global warming trend since the beginning of the 21st century, leading to a slowdown in global mean surface temperature warming rate to 0.02-0.09°C (Xie and Kosaka, 2017). Several studies have shown that this has coincided with the negative phase of the Pacific Decadal Oscillation and has been largely attributed to the internal variability over the Pacific Ocean (Kosaka and Xie, 2013, 2016; Trenberth and Fasullo, 2013; England et al., 2014). The extreme El Niño of 2015 brought about the end of the global warming hiatus (Hu and Fedorov, 2017). This cooling trend is more prominent during the boreal winter months (Trenberth et al., 2014).

With the end of the global warming hiatus, the North Atlantic Ocean emerged as an important driver of the interannual variability of $DA_{\%}$ over South Asia during 2011-2018. A few recent studies have shown that since late 1970s the Atlantic Ocean has assumed increasing influence over the climate of the Asian monsoon region as the influence of the tropical Pacific has reduced (Kucharski et al., 2007; Sabeerali et al., 2019; Srivastava et al., 2019). This in-turn impacts the circulation responsible for dust uplift and transport. The spatial pattern of correlation between $DA_{\%}$ and SST for 2011-2018 in Fig. 4b shows resemblance to SST tripole pattern resulting from surface heat exchanges during the positive phase of NAO (Bjerkness, 1964; Visbeck et al., 2001; Rodwell et al., 1999; Han et al., 2016). In general, the positive phase of NAO projects to positive SST anomaly over the mid-latitude North Atlantic and negative SST anomalies over the sub-tropical and the sub-polar North Atlantic (also see Supplementary Fig. S2 a-c). $DA_{\%}$ is significantly correlated with the regions associated with these mid-latitude (Region 1 in Fig. 4b) and sub-tropical (Region 2 in Fig. 4b) arms of the SST tripole. This tripole have recently changed sign from being negative (warm phase) during 2001-2010 to positive (cold phase) during 2011-2018 (Supplementary Fig. S2 d-e). That is, during 2011-2018, SST over North Atlantic shows a decreasing trend in the sub-tropics (centered on 20°N latitude), which is not significant, a significant (at 95% confidence level) increasing trend over the mid-latitude (centered on 40°N latitude) and again a significant decreasing trend in the subpolar region (centered on 60°N latitude, dashed boxes in Fig. 5b). The SST trends over the North Atlantic during 2001-2010, on the other hand, are not significant. In fact, December-February NAO index was neutral to negative during 2001-2010 (average NAO index -0.4) and changed to positive during 2011-2018 (average NAO index 2.4) (Delworth et al., 2016; Iles and Hegerl, 2017) in tune with the switch in the sign of SST tripole during this period (Fig. 5c). However, as is shown in Section 3.3, during 2011-2018 there has also been a change in the relation between the North Atlantic SST anomalies, NADI and NAO, which remotely impacts circulation over South Asia. Thus, to sum up, with the resumption of global warming, the North Atlantic SST seems to assume importance in controlling dust activity over South Asia, indicating a shift from the well-known importance of the Pacific SST. ~~The linkage is through a persistent positive phase of NAO during 2011-2018 and its imprint on the North Atlantic SST tripole, the latter being in its positive (cold) phase during this period.~~ This takes place during a persistent positive phase of NAO and positive (cold) phase of the North Atlantic SST tripole. In the following sections we show how the Pacific Ocean influence on the circulation controlling South Asian dust is reduced during 2011-2018. This is followed by a discussion on the physical mechanism responsible for North Atlantic SST leading to increased South Asian dust activity during this period.

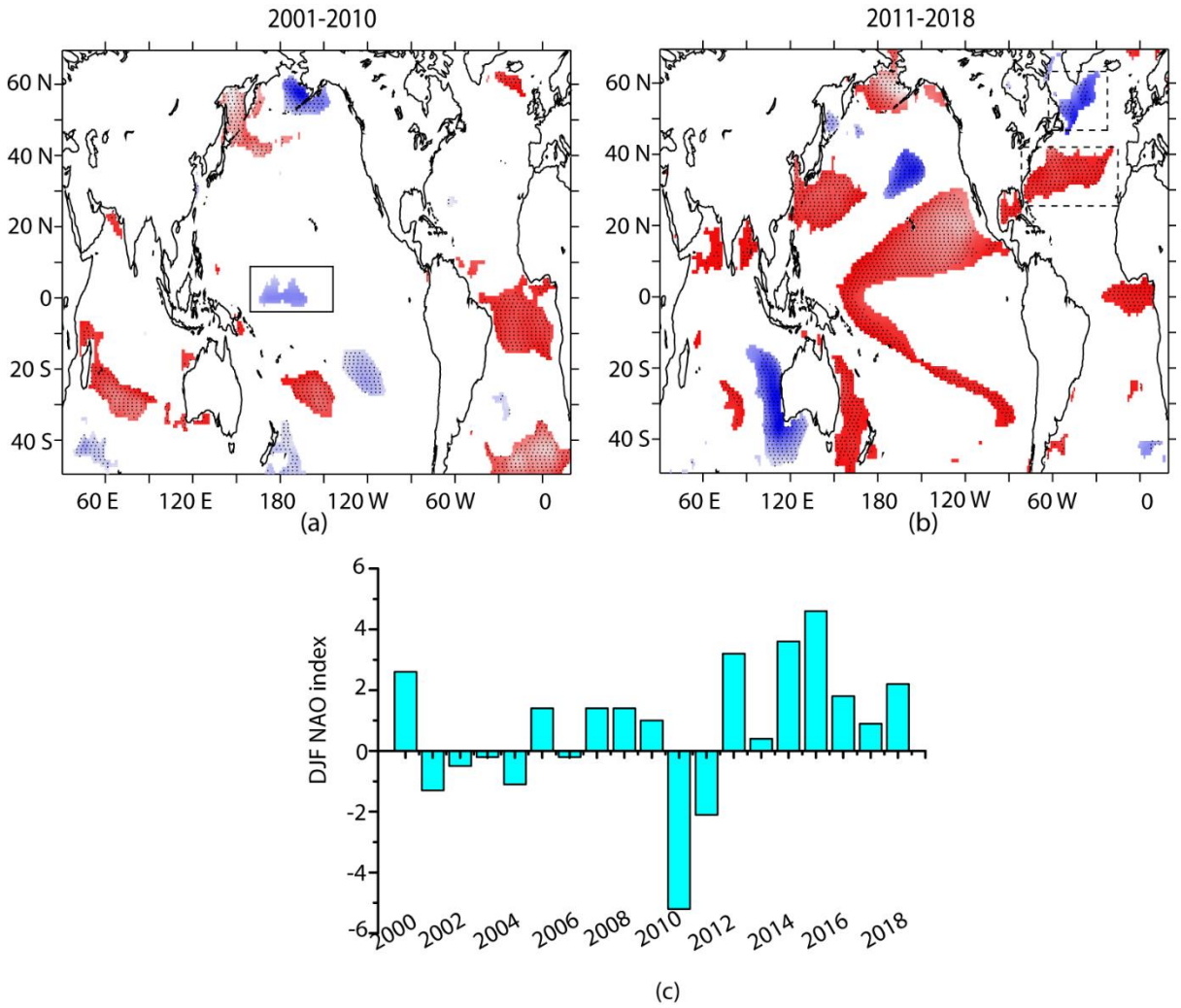

Figure 5: Regions experiencing positive (red shades) and negative (blue shades) trends in sea surface temperature during (a) September-October of 2001-2010 and (b) April-June of 2011-2018 significant at 90% confidence level. The overlaid black stippling shows the regions where the trend is significant at 95% confidence level. (c) Time series of December-February Hurrell's station-based NAO index for 2000-2018.

3.2 Reduced influence of the Pacific Ocean on South Asian dust

Several studies have linked warming of the central equatorial Pacific Ocean, associated with the developing phase of an El Niño, to weak monsoon over South Asia and drought (e.g., Kumar at al., 2006; Ashok et al., 2007; Wang et al., 2015). This is due to the shifts in the Walker circulation leading to anomalous ascending motion over the warm SST region and compensating descending motion over South Asia. In Figs. 6 a-b we can see such signatures of weakening of monsoon induced by central equatorial Pacific ~~(taken as 175-140°W longitude, 5°N-5°S latitude)~~ SST warming during September-October months of 2001-2010. This is characterized by anomalous lowering of the 200-hPa geopotential height over South Asia during May-September due to reduced diabatic heating. There is anomalous near-surface northerly wind over the northern IO and negative precipitation anomalies over large part of India and surroundings. The negative precipitation

anomalies over northwest India, Pakistan, and Afghanistan along with anomalous northwesterly at 850-700 hPa over the Indo-Gangetic Plain are most relevant to increased dust emission, transport, and longer atmospheric residence time due to less wet depositions. In contrast, during 2011-2018, central Pacific SST does not have any significant impact on geopotential height and precipitation over the dust belt of South Asia (Figs. 6c-d). This points to a weakening relation between central Pacific SST and atmospheric circulation over South Asia. The northwesterly wind anomaly induced over some parts of the Indo-Gangetic Plain during this period overlaps partially with dust source regions. Overall, it appears that dryness due to suppression of precipitation over large area plays an important role compared to anomalous wind in the lower-to-mid troposphere. Partial correlation between annual averaged central equatorial Pacific SST and $DA_{\%}$ adjusted for annual NADI gives a correlation coefficient of 0.64 during 2001-2010, which is significant at 95%. However, for the period 2011-2018, the partial correlation only yields a value of -0.23.

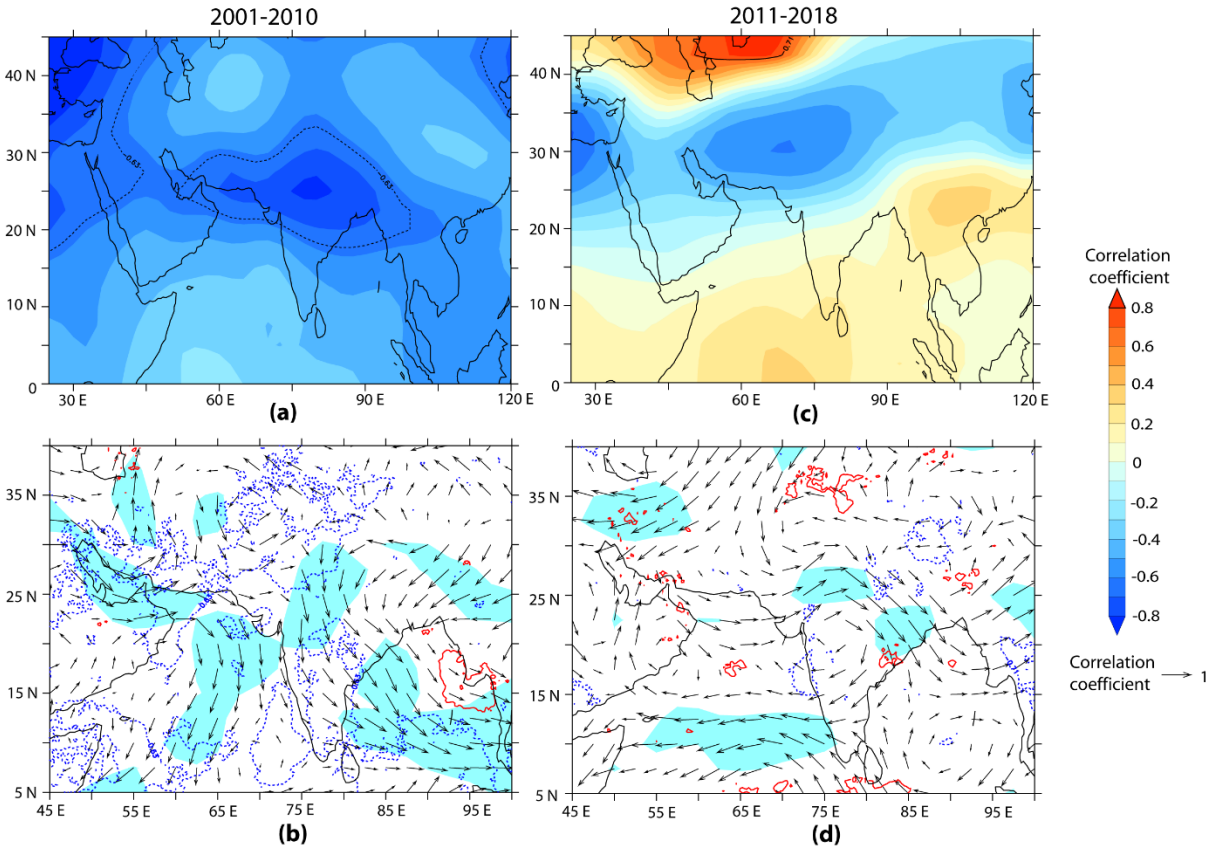

Figure 6: Correlation between September-October central equatorial Pacific SST and different meteorological parameters averaged for May-September for (left panels) 2001-2010 and for (right panels) 2011-2018. (a) and (c) Shading shows correlation between Pacific SST and geopotential height at 200 hPa pressure level and the contours enclose the regions where correlations are significant at 95%. (b) and (d) Continuous red (dashed blue) contours enclose regions having positive (negative) correlation between Pacific SST and precipitation significant at 95% confidence level. Arrows show correlation between Pacific SST and wind vectors averaged over 850-700 hPa pressure levels. Light blue shade highlights the regions where one of the components of the wind vector has significant (at 95%) correlation.

3.3 Physical Mechanism linking South Asian dust with Atlantic SST

The observations in Section 3.1 invoke the question: what could be the possible mechanism by which the changes in the North Atlantic SST impact South Asian dust activity during 2011-2018, when the Pacific Ocean influence has reduced? The 'April to June North Atlantic Difference Index' (NADI, described in Section 3.1) is more strongly and persistently correlated to winter and spring NAO index during 2001-2010 than during 2011-2018 (Fig. 7). This indicates that, although persistent positive phases of NAO and SST tripole is observed, the relation between winter and spring NAO and NADI (via SST tripole) has changed during 2011-2018~~,~~. This ~~which~~ has impacted circulation over South Asia and, thereby, dust load. To understand the mechanism involved, we have estimated the correlation between April-June NADI and different meteorological fields averaged for the months May-September when NADI is significantly correlated with $DA_{\%}$ (see Fig. 4~~c~~d) and also when high dust activity is widespread over South Asia. The results in Fig. 8 reveal that during 2001-2010, NADI projects on to a cyclonic circulation anomaly at ~~850-700~~ 500-200 hPa pressure level northwest off the British Isles (red box in Fig. 8a) and a tripole-like SST anomaly with warming in the Norwegian Sea (Fig. 8b). This resembles the Summertime East Atlantic (SEA) pattern, which is the second dominant mode of variability after NAO over the North Atlantic Ocean during summer (Wulff et al., 2017; Osso et al., 2018; Osborne et al., 2020), although, there are certain differences: (1) the cold sub-polar arm of the SST tripole has greater southward extension (Fig. 8b) and (2) an additional positive sea level pressure anomaly along western North Atlantic between 10°N-50°N latitude is detected (Fig. 8c). The cyclonic circulation anomaly extends through the entire depth of the troposphere (not shown) and emanates eastward propagating wavetrain (Borah et al., 2020), as indicated by anomalies of the meridional wind in Fig. 8a. Anticyclonic circulation over Southwest Asia associated with the wavetrain translates to anomalous near-surface northerly over the central Indo-Gangetic Plain and the Bay of Bengal (Fig. 9a). This signals a weakening of SWM circulation. Velocity potential at 850 hPa pressure level (green contours in Fig. 8c) during May-September of 2001-2010 points to large-scale descending motion and divergence over the North Atlantic. This is associated with negative precipitation anomalies over the cooler SST regions of the North Atlantic, as well as, over Sahel (green contours in Fig. 8b). The impact of NADI over South Asia is mostly felt through the reduction in precipitation over west India and westerly anomalies in the south-central Indo-Gangetic plain. Negative precipitation anomalies are also present over the dust source regions of the Middle East and southern part of Central Asia.

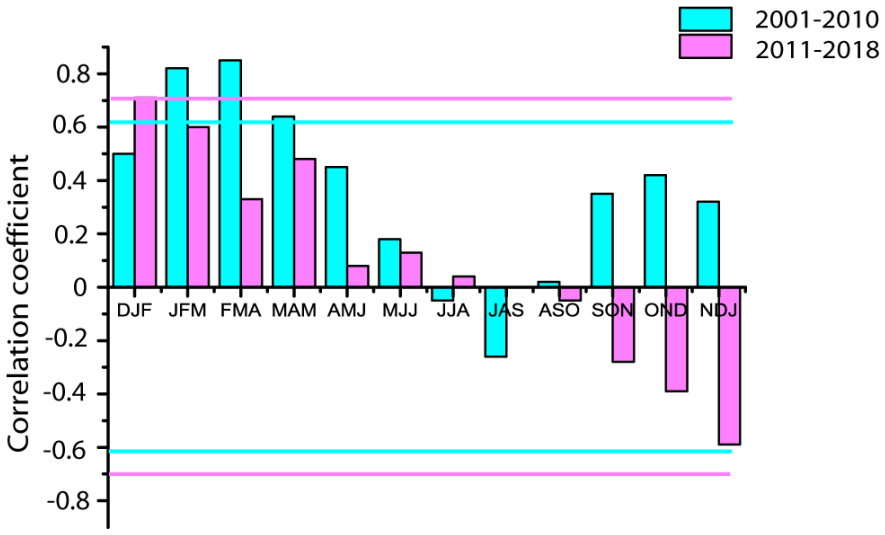

Figure 7: Correlation between seasonal NAO index and April-June North Atlantic Difference Index (NADI) separately for 2001-2010 and 2011-2018. The blue and pink horizontal lines indicate the 95% confidence levels for 2001-2010 and 2011-2018 respectively.

During 2011-2018, the significant imprint of NADI on SEA wind pattern northwest off the British Isles is absent, along with a weakening of the eastward propagating wavetrain (Fig. 8d), implying a shift in the relation between them. The anomalous southwesterlies over the eastern part of the Caspian Sea is replaced by anomalous northerlies. Near the surface level, this translates to stronger northerlies and northwesterlies over the dust source regions of southwest Asia and northwest India (Fig. 9b). With the North Atlantic SST tripole changing sign from warm during 2001-2010 to cold during 2011-2018 (Supplementary Fig. S2 d-e), NADI is significantly correlated with the mid-latitude and sub-tropical arms of the SST tripole, but not with the sub-polar arm of the SST tripole (shading in Fig. 8e). Additionally, there is an eastward shift in the region of positive correlation between NADI and the mid-latitude arm of the tripole and a southward shift in the region of negative correlation between NADI and the sub-tropical arm of the tripole. The region of low pressure off the British Isles, seen during 2001-2010, is absent during 2011-2018 (Fig. 8f) due to the absence of the SEA pattern. Instead, a large region of positive correlation between NADI and sea level pressure over the sub-tropical North Atlantic appears (Fig. 8f). Correlating the north and south boxes of NADI separately with sea level pressure shows that the combined effect of SST warming over the northern box and SST cooling over the southern box leads to this anomalous high sea level pressure (Supplementary Fig. S3). The northern box coincides with the location of the Azores high, which forms the northern part of the descending branch of the Hadley cell. Anomalous SST warming in this region, through overlying mass redistribution, can induce anomalous descending motion and increase SLP in the tropics. Since SST over mid-latitude North Atlantic showed significant positive trend during 2011-2018, as opposed to the period 2001-2010, the impact of the SST over the north box of NADI on the sea level pressure is pronounced during 2011-2018. The eastward extension of anomalous warm mid-latitude SST has resulted in convergence, as indicated by 850 hPa velocity potential (green contours in Fig. 8f), and positive precipitation anomaly over the Mediterranean region including North Africa and northwestern part of the Arabian Peninsula (green contours in Fig. 8e). Additionally, warming (cooling) in the tropical North Atlantic SST can induce a compensatory descending (ascending) motion over the Mediterranean region (Sun et al., 2009). The summertime wet anomaly over the Mediterranean region leads to anomalous descending motion

over South Asia, Middle East and East Africa, which is indicated by negative velocity potential at 850 hPa over this region (Fig. 8f). The net effect is that the region of positive sea level pressure anomalies now stretches to encompass the Sahel, Middle East, western India and the central part of northern IO (orange shading in Fig. 8f). Over South Asia this development suppresses the southwest monsoon circulation and precipitation over different regions of India and leads to general dryness. Together, a weakening of the southwest monsoon circulation and development of anomalous dust-bearing northerlies/northwesterlies over southwest Asia and northwest India drives an active dust season over South Asia. ~~More importantly, as seen by the vectors in Fig. 8d, the positive sea level pressure anomaly over the Middle East invigorates the westerlies carrying dust from Southwest Asia to South Asia. The northerlies which are important for dusty weather over Pakistan-Afghanistan-Iran are also strengthened.~~

In summary, although persistent positive phase of NAO prevailed during 2011-2018, a disassociation between NAO and NADI, via changes in the North Atlantic SST anomaly pattern, influenced circulation over the Eurasian sector and over North Africa. Over South Asia and surroundings, this projected to weakening of the Atlantic wavetrain, increased subsidence and positive anomalies of sea level pressure, which resulted in general weakening of the monsoon and strengthening of the dust-transporting northerlies and westerlies.

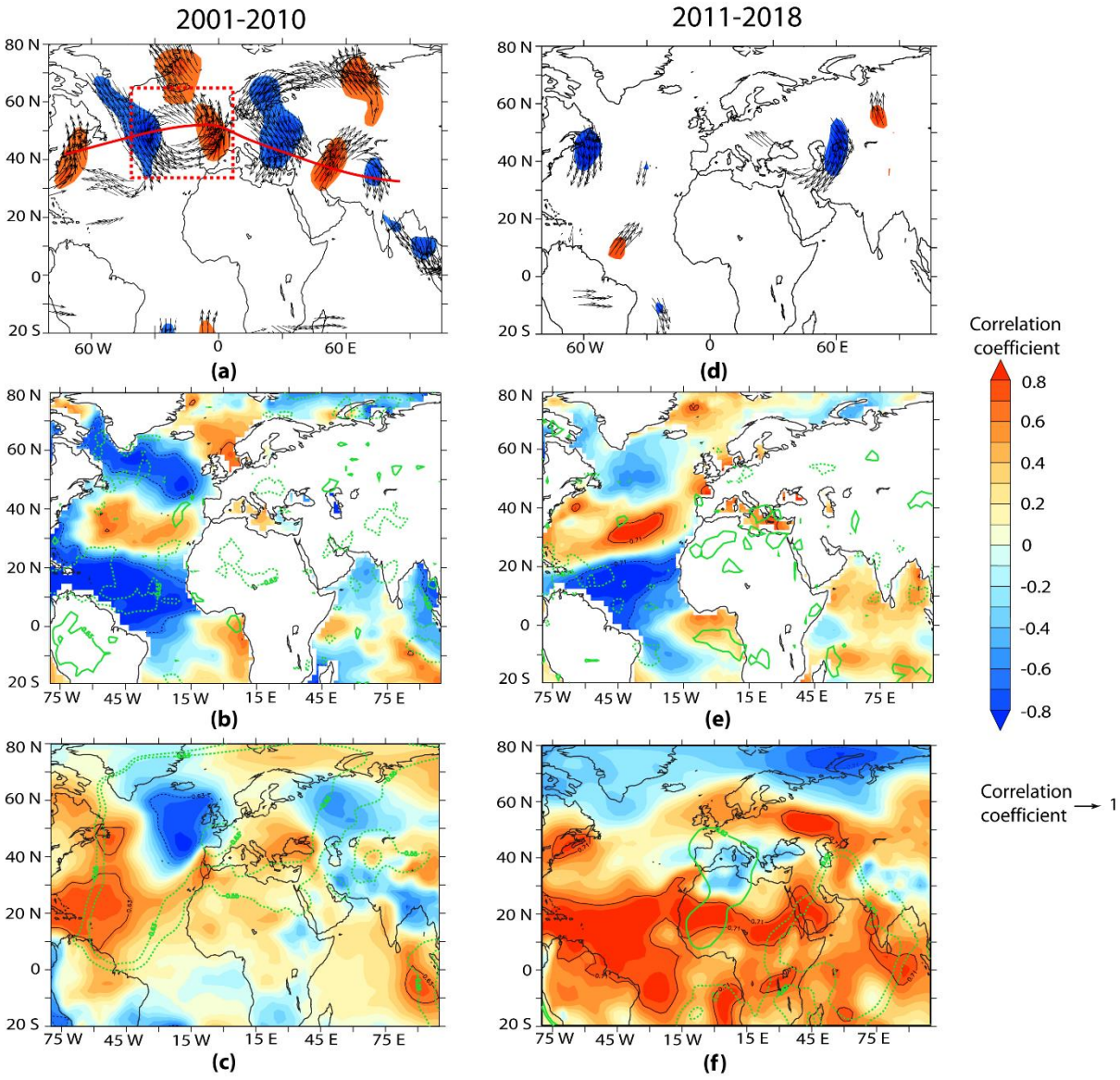

Figure 8: Correlation between the April-June North Atlantic Difference Index (NADI) and different meteorological parameters from NCEP/NCAR Reanalysis averaged for May-September for (left panels) 2001-2010 and (right panels) 2011-2018. (a) and (d) Arrows show correlation between NADI and wind vectors averaged between 500~~850~~ and 200~~700~~ hPa pressure levels significant at 95%. ~~Light~~ Red and blue shade~~s~~ highlight~~s~~ the regions where ~~one of~~ the meridional component~~s~~ of the wind ~~vector~~ has significant ~~is significantly~~ (95% confidence level) positive and negative correlation~~s~~~~ed~~, respectively, with NADI. (b) and (e) Shading shows correlation between NADI and SST and the green contours enclose the regions where significant correlation (at 95% level) exists between NADI and precipitation. Black contours indicate the regions where correlation between NADI and SST are significant at 95%. (c) and (f) Shading shows correlation between NADI and sea level pressure and the green contours enclose the regions where significant correlation exists between NADI and velocity potential at 850 hPa pressure level: inner and outer contours indicate 95% and 90% confidence levels respectively. Black contours indicate the regions where correlation between NADI and sea level pressure are significant at 95% level. For all the panels continuous and dashed contours are indicative of significant positive and negative correlations respectively.

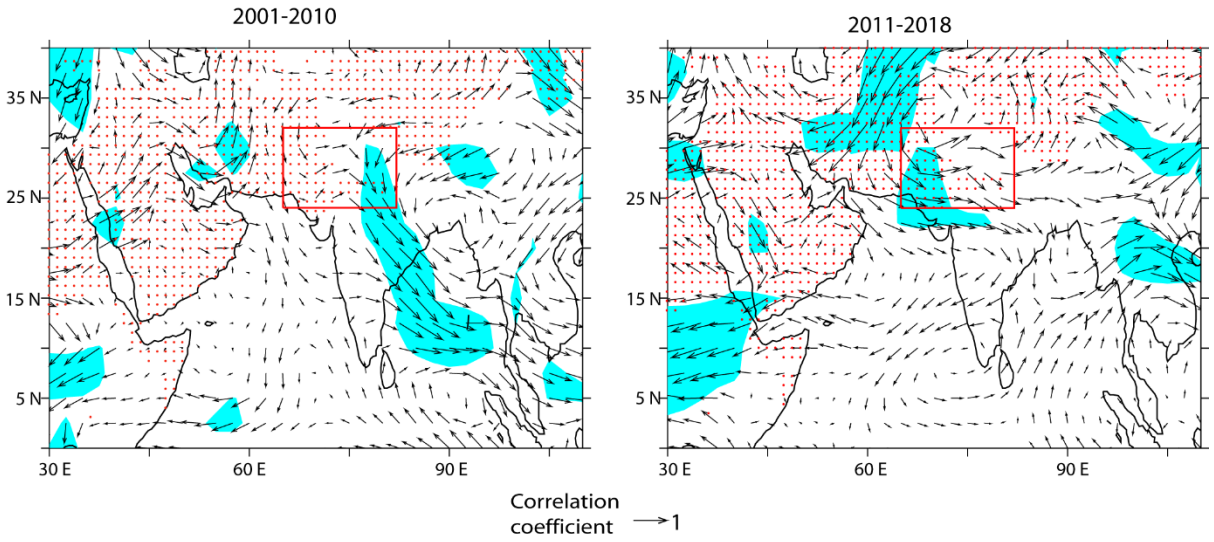

Figure 9: Correlation between the April-June North Atlantic Difference Index (NADI) and wind averaged over 700-850 hPa for May-September for (left panels) 2001-2010 and for (right panels) 2011-2018. Light blue shade highlights the regions where one of the components of the wind vector is significantly (95% confidence level) correlated with NADI. Red stippling show dust emission regions obtained from CESM model simulations, and the red square encloses South Asian dust belt considered in this study.

3.4 CESM simulation of Atlantic Ocean influence

The teleconnection between the North Atlantic SST and dust load over South Asia is explored further with the help of CESM simulations, with a view to isolate the contributions from North Atlantic SST anomalies. To achieve this, we have compared two sets of simulations, as explained in Section 2.2, for ten model years: one with climatological SST (Ctrl run) and the other with the SST trend for 2011-2018 superposed on the climatological SST over the North Atlantic (NAtl run). The difference (NAtl – Ctrl runs) yields the contribution solely from North Atlantic SST anomalies. It is important to note here that while NADI reflects the gradient between the mid-latitude and sub-tropical branches of North Atlantic SST, SST anomalies imposed for the NAtl run illustrate the response due to spatial pattern of SST anomalies over the entire North Atlantic due to persistent positive phase of NAO. As discussed in Section 2.3, although there are certain limitations, CESM can reproduce the main aspects of atmospheric circulation and the spatial and temporal characteristics of dust over South Asia quite well. This gives us confidence in using the model for our present study.

The differences between NAtl and Ctrl simulations for May-September are shown in Fig. ~~9~~10, which highlights that the North Atlantic SST anomaly, similar to during 2011-2018, can modulate South Asian dust activity via a combination of reduced precipitation over the northern IO and strengthening of the dust-bearing northwesterlies over the dust source regions. Cold SST tripole anomaly results in cooling in the upper troposphere and lowering of the geopotential heights over South and Southwest Asia; both of which are important indicators of a weak South Asian monsoon circulation (Fig. 10~~9~~a). An east-west wave train over the mid-latitude and sub-polar region of Eurasia sets-in with anticyclonic circulation over the sub-polar and cyclonic circulations over the mid-latitude North Atlantic and also over the British Isles (Fig. 10~~9~~b). Furthermore, a positive anomaly of sea level pressure extends eastwards from the sub-tropical North Atlantic and is particularly strong over the northern IO. These anomalies are similar to the response of the sea level pressure to NADI seen in the tropics; but are opposite to that seen north of the mid-latitudes (Fig. 8f). Previously, model simulations have shown that the

tropical North Atlantic SST opposes the response of sea level pressure to the extra-tropical part of the cold SST tripole (Osborne et al., 2020). A cyclonic circulation over the central equatorial IO and an anticyclonic circulation over the northwestern IO inhibit the inflow of moisture into much of the Indian subcontinent leading to deficit rainfall. It is the westerlies, which form the northern branch of the anticyclone, that transport dust from the South Asian sources. For May-September, maximum increase in dust optical depth (τ_d) due to SST tripole is located over the South Asian dust source region with dust emissions from the Thar being the main contributor (Fig. 10~~9~~c). While over the dust source regions the increase in τ_d is within 10%, dust transport by the strengthened westerlies can lead up to 20% increase in τ_d in the eastern Indo-Gangetic plain. Simultaneously, anomalous southerlies and southeasterlies over the Arabian Peninsula suppress dust activity in the region (Fig 10~~9~~b and c). The peak increase in τ_d over South Asia due to North Atlantic SST is observed during June, when ~30% increase in τ_d compared to CESM-simulated climatological values is achieved over the South Asian dust source regions (Fig. 10~~9~~d). To test the significance of the positive anomalies of τ_d, we carried out Monte Carlo calculations by randomly selecting 6 years from NAtl and Ctrl simulations and differencing the τ_d. By repeating this procedure 600 times, we find that in 90% cases NAtl-Ctrl yields positive anomalies of τ_d. It is important to note that although there is a rainfall deficit over South Asia and the northern IO, only a small area within the main dust source regions is impacted. This implies that a general increase in dryness and τ_d due to cold phase of North Atlantic SST tripole is widespread over South Asia. However, the strengthened westerlies are responsible for enhanced dust flux over the dust belt of South Asia. In this context, it is also worth mentioning that earlier works have reported that cooling over the North Atlantic, either associated with the cold phase of Atlantic Multidecadal Oscillation or due to the slowdown of the Atlantic Meridional Oscillation, is associated with weakened monsoon (e.g., Goswami et al., 2006; Zhang and Delworth, 2006; Feng and Hu, 2008; Liu et al., 2020). At decadal scale, rainfall data for 1901-2004 showed that the positive (cold) phase of the SST tripole is associated with excess monsoon over India due to strengthening of the westerlies over the northern IO (Krishnamurthy and Krishnamurthy, 2015). However, the sign of correlation between the South Asian monsoon and the SST tripole has undergone changes since 2000 with the negative (warm) phase of the SST tripole being associated with strong monsoon over South Asia and vice versa (Gao et at., 2017), implying interdecadal shifts in the relation between the two. These observations are supportive of our arguments above.

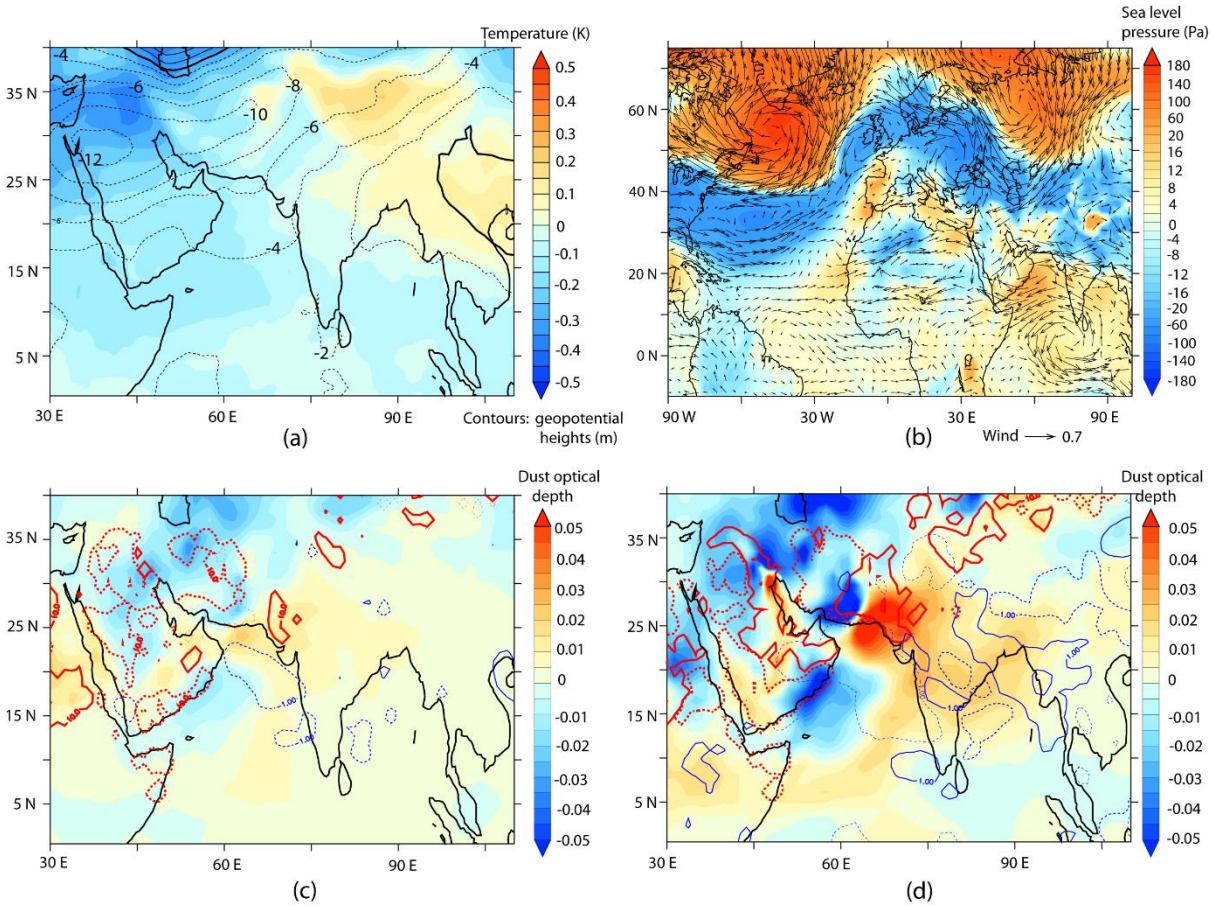

Figure 109: Differences between CESM-NAtl and CESM-Ctrl simulations for (a-c) May-September. (a) Shading and contours indicate differences in temperature and geopotential height respectively at 200 hPa pressure level. (b) Shading indicates difference in sea level pressure and the arrows indicate difference in wind vectors at 850 hPa pressure level. (c) Difference in dust optical depth over the northern Indian Ocean and surrounding regions are shown by shading. The thick red contours enclose the regions where dust emission flux difference is greater than 10 mg m^2 day^{-1} and the thin blue contours enclose the regions where precipitation difference is greater than 1 mm day^{-1}. (d) Same as (c) but for the month of June. For all contours, positive values are shown by continuous lines and negative values are shown by dashed lines.

The increase in τ_d discussed above is enabled by strengthening of dust-transporting westerlies at 800 hPa pressure level, which can, averaged for May to September, increase dust concentration by 20% at this altitude. This furthers when we analyse month-by-month changes in dust transport, as shown in Fig. 110, where a much stronger influence of North Atlantic SST tripole on dust concentrations is evident. The positive anomalies of dust concentration slowly start to build up during April to reach a peak during June and then subside by September. During May and June, the North Atlantic SST tripole can enhance dust concentration by 40-50% in the lower and mid-troposphere over the South Asian dust belt. These are also the months when maximum negative anomalies of precipitation are seen, following which positive anomalies of precipitation builds up. During May, maximum dust concentration anomaly centered on 800 hPa pressure level is associated with transport from the eastern Arabian Peninsula (due to anomalous southwesterly). During June, on the other hand,

the strengthened northerlies transport dust all the way from eastern part of Central Asia into South Asia between 60°E-75°E longitudinal belts. Additionally, descending motion above 500 hPa pressure level leads to trapping of dust below this level. The overall weakening of the South Asian monsoon circulation is also demonstrated by the anomalous upper-level westerlies.

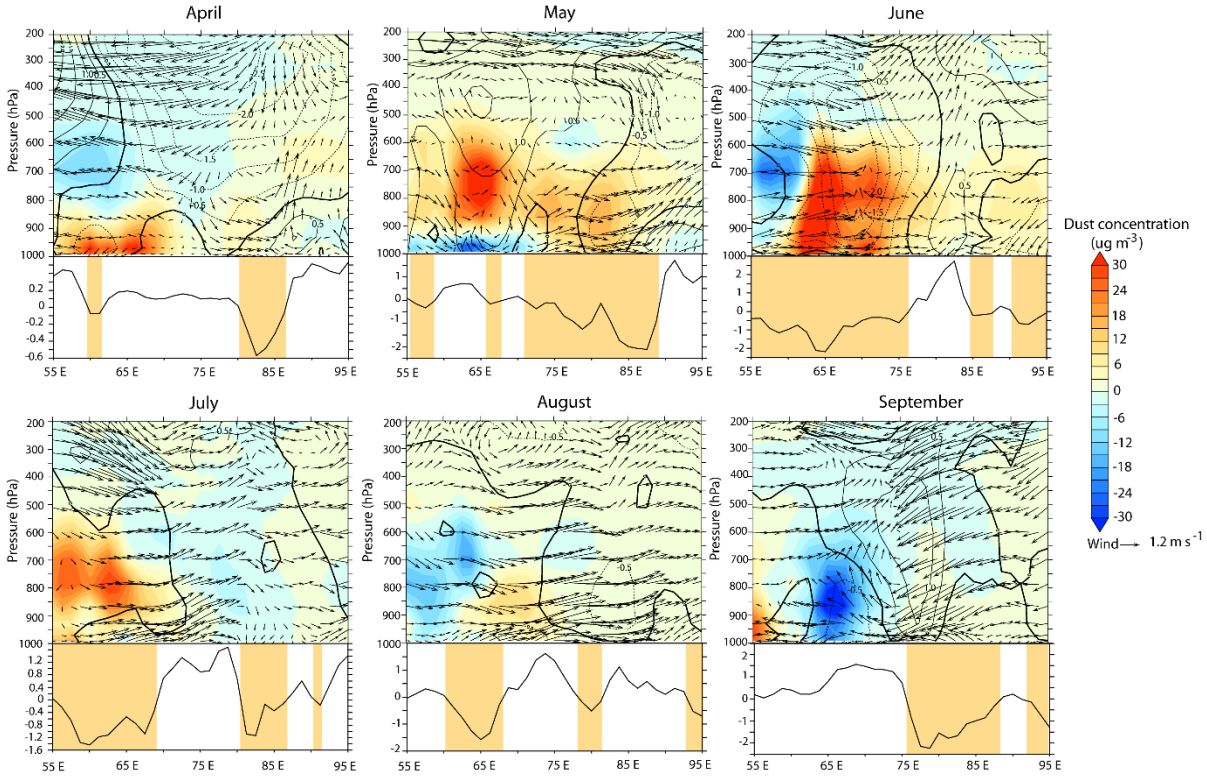

Figure 1~~0~~: Sections along 25°N latitude illustrating month-wise differences in dust transport between CESM-NAtl and CESM-Ctrl simulations. In upper part of each panel, shadings indicate difference in dust concentrations between the two simulations, the vectors are the differences in zonal and vertical components of wind and the contours are the differences in meridional component of wind. Continuous (dashed) contours indicate southerly (northerly) wind anomalies. The lower part of each panel plots precipitation differences, in mm day^{-1}, between CESM-NAtl and CESM-Ctrl simulations along 25°N latitude. The orange shades indicate the longitudinal belts which have negative anomalies of precipitation. Note that the vertical velocity is expressed as Pa s^{-1} and has been multiplied by 40.

4 Conclusions

Our study underlines the need to look at large-scale factors, which are global in nature, in significantly modulating dust load over South Asia, in addition to changes in local factors. This is specifically relevant considering that about 50% of dust over this region is transported from remote (non-local) sources (Banerjee et al., 2019). In this light, we have attempted to understand how changes in large-scale SST patterns can impact dust emissions and transport pathways in this region. The "memory" of SST provides a bridge between the circulation changes taking place across the globe. Our study relies on satellite data which are only available since 2001. Even with this we see significant changes in terms of the relative importance of SST from different regions in driving interannual variability of dust over South Asia.

Our study shows that during the second decade of the 21st century the North Atlantic SST has emerged as a dominant player in controlling dust activity over South Asia, in contrast to the hitherto important role played by the Pacific SST. During the global warming hiatus period of 2001-2010, SST over the equatorial central Pacific Ocean modulated the strength of the South Asian summer monsoon and, by extension, dust levels. From 2011 onwards, persistent positive phases of NAO resulted in positive (cold) phase of the North Atlantic SST tripole pattern. During this period~~Specifically~~, high dust activity ~~during 2011-2018~~ is associated with negative SST anomaly over sub-tropical North Atlantic and positive SST anomaly over mid-latitude North Atlantic, the regions corresponding to the two southern arms of the North Atlantic SST tripole. The difference in SST between these two regions, which we term as North Atlantic Difference Index or NADI, projects into the SEA-like circulation anomaly and eastward propagating wavetrain during May to September months of 2001-2010. Interestingly, changes in the pattern of the North Atlantic SST anomalies during 2011-2018 weakened ~~during 2011-2018 a weakening of~~ the relation between NAO and NADI and ~~dilute~~also diluted~~s~~ the impact of NADI on SEA. The result is a weakening of the South Asian monsoon circulation and development of anomalous dust-transporting northwesterlies and northerlies. This is facilitated by a weakening of the wavetrain from the North Atlantic and positive sea level pressure anomalies extending from the tropical North Atlantic into the northern IO ~~which leads to decreased precipitation and general increase in dryness with enhanced dust load. Additionally, positive sea level pressure anomaly over South and Southwest Asia leads to anomalous northerlies and westerlies which are responsible for transporting dust over South Asia.~~ Sensitivity studies conducted with CESM model shows that averaged for May-September the North Atlantic SST tripole anomaly can lead to around 10% increase in dust optical depth, while it can contribute to 30% increase in dust optical depth during the month of June. Most of the increase in dust load can be attributed to enhanced transport at 800 hPa pressure level, which increases dust concentration by 20% for May-September and by as much as 40-50% during May-June.

The present study demonstrates impact of the North Atlantic Ocean using 18 years of satellite data. However, in the past, cold events in the North Atlantic have been associated with the slowdown of the South Asian monsoon system and increase in dust fluxes over the northern Indian Ocean and Southwest Asia (e.g., Pourmand et al., 2004; Mohtadi et al., 2014; Safaierad et al., 2020). Longer term data needs to be analysed from recent past to better understand how this relation between dust and North Atlantic SST has fluctuated over time. This will provide important clues as to how future relative changes in global SST in a warming world can control dust fluxes over South Asia and the possible climate implications.

Code availability

The code for CESM1.2 is available at https://www.cesm.ucar.edu/models/cesm1.2/

Data availability

Level 3 MODIS Aqua+Terra version 6.1 daily aerosol data was downloaded from Level 1 and Atmosphere Archive and Distribution System (LAADS) Distributed Active Archive Center (DAAC) website (https://ladsweb.modaps.eosdis.nasa.gov/missions-and-measurements/science-domain/l3-atmosphere). IASI dust

optical depth was obtained from https://iasi.aeris-data.fr/dust-aod_iasi_a_data/. NCEP/NCAR meteorological fields, NOAA ERSST version 5 data, OISST version 2, COBE SST version 2 data and GPCP version 2.3 precipitation data were obtained from National Oceanic and Atmospheric Administration (NOAA) Physical Sciences Laboratory website (https://psl.noaa.gov/data/gridded/data.ncep.reanalysis.html). Monthly PERSIANN precipitation data is maintained at University of California, Irvine (UCI), Center for Hydrometeorology and Remote Sensing (CHRS) website (https://chrsdata.eng.uci.edu/). Hurrell's station-based NAO data is available at https://climatedataguide.ucar.edu/climate-data/hurrell-north-atlantic-oscillation-nao-index-station-based. AERONET coarse mode aerosol data were obtained from https://aeronet.gsfc.nasa.gov/.

Author contribution

PB conceived the study, carried out model simulations, analyzed the data and wrote the manuscript. SKS and KKM contributed to scientific analysis and revision of the manuscript.

Competing interests

The authors declare that they have no conflict of interest.

Special issue statement

This article is part of the special issue "Interactions between aerosols and the South West Asian monsoon". It is not associated with a conference.

Acknowledgements

This research is supported by the Ministry of Earth Sciences (grant no. MM/NERC-MoES-1/2014/002). PB is also supported by Department of Science and Technology INSPIRE Faculty scheme. We acknowledge the computational facilities provided by Supercomputer Education and Research Centre (SERC) at the Indian Institute of Science for carrying out CESM simulations.

References

Abish, B. and Mohanakumar, K.: Absorbing aerosol variability over the Indian subcontinent and its increasing dependence on ENSO, Global Planet. Change, 106, 13–19, https://doi.org/10.1016/j.gloplacha.2013.02.007, 2013.

Albani, S., Mahowald, N. M., Perry, A. T., Scanza, R. A., Heavens, N. G., Zender, C. S., Maggi, V., Kok, J. F., and Otto-Bliesner, B. L.: Improved dust representation in the Community Atmosphere Model. J. Adv. Model. Earth Syst., 6, 541–570, https://doi.org/10.1002/2013MS000279, 2014.

Annamalai, H., Taguchi, B., McCreary, J. P., Nagura, M., and Miyama, T.: Systematic errors in South Asian monsoon simulation: Importance of equatorial Indian Ocean processes, J. Climate, 30, 8159–8178, https://doi.org/10.1175/JCLI-D-16-0573.1, 2017.

Ashok, K., Guan, Z., and Yamagata, T.: Impact of the Indian Ocean dipole on the relationship between the Indian monsoon rainfall and ENSO, Geophys. Res. Lett., 28, 4499–4502, https://doi.org/10.1029/2001GL013294, 2001.

Ashok, K., Guan, Z., Saji, N. H., and Yamagata, T.: Individual and combined influences of ENSO and the Indian Ocean Dipole on the Indian Summer Monsoon, J. Climate, 17, 3141–3155, https://doi.org/10.1175/1520-0442(2004)017<3141:IACIOE>2.0.CO;2, 2004.

Ashok, K., Behera, S. K., Rao, S. A., Weng, H. Y., and Yamagata, T.: El Niño Modoki and its possible teleconnection, J. Geophys. Res.-Oceans, 112, C11007, https://doi.org/10.1029/2006JC003798, 2007.

Ashouri, H., Hsu, K., Sorooshian, S., Braithwaite, D. K., Knapp, K. R., Cecil, L. D., Nelson, B. R., and Pratt, O. P.: PERSIANN-CDR: daily precipitation climate data record from multisatellite observations for hydrological and climate studies, B. Am. Meteorol. Soc., 96, 69–83, https://doi.org/10.1175/BAMS-D-13-00068.1, 2015.

Barlow, M., Heidi, C., and Bradfield, L.: Drought in Central and Southwest Asia: La Ninã, the Warm Pool, and Indian Ocean Precipitation, J. Climate, 15, 697–700, 2002.

Banerjee, P., and Kumar, S. P.: ENSO Modulation of Interannual Variability of Dust Aerosols over the Northwest Indian Ocean, J. Climate, 29, 1287–1303, https://doi.org/10.1175/JCLI-D-15-0039.1, 2016.

Banerjee, P., Satheesh, S. K., Krishnamoorthy, K., Nanjundiah, R. S., and Nair, V. S.: Long-Range Transport of Mineral Dust to the Northeast Indian Ocean: Regional versus Remote Sources and the Implications, J. Climate, 32, 1525–1549, https://doi.org/10.1175/JCLI-D-18-0403.1, 2019.

Bjerknes, J.: Atlantic air-sea interaction, Adv. Geophys. 10, 1–82 https://doi.org/10.1016/S0065-2687(08)60005-9, 1964.

Bollasina, M. A., Ming, Y., and Ramaswamy, V.: Anthropogenic aerosols and the weakening of the South Asian summer monsoon, Science, 334, 502–505, https://doi.org/10.1126/science.1204994, 2011.

Boos, W. R. and Hurley, J. V.: Thermodynamic Bias in the Multimodel Mean Boreal Summer Monsoon, J. Climate, 26, 2279–2287, https://doi.org/10.1175/jcli-d-12-00493.1, 2013.

Borah, P. J., Venugopal, V., Sukhatme, J., Muddevihal, P., and Goswami, B. N.: Indian monsoon derailed by a North Atlantic wavetrain, Science, 370, 1335–1338, doi: 10.1126/science.aay6043, 2020.

Capelle, V., Chédin, A., Pondrom, M., Crevoisier, C., Armante, R., Crepeau, L., and Scott, N.: Infrared dust aerosol optical depth retrieved daily from IASI and comparison with AERONET over the period 2007–2016, Remote Sens. Environ., 206, 15–32, https://doi.org/10.1016/j.rse.2017.12.008, 2018.

Chang, C., Harr, P., and Ju, J.: Possible Roles of Atlantic Circulations on the Weakening Indian Monsoon Rainfall–ENSO Relationship, J. Climate, 14, 2376–2380, https://doi.org/10.1175/1520-0442(2001)014<2376:PROACO>2.0.CO;2, 2001.

Chattopadhyay, R., Phani, R., Sabeerali, C. T., Dhakate, A. R., Salunke, K. D., Mahapatra, S., Suryachandra Rao, A., and Goswami, B. N.: Influence of extratropical sea-surface temperature on the Indian summer monsoon: An unexplored source of seasonal predictability, Quart. J. Roy. Meteor. Soc., 141, 2760–2775, https://doi.org/10.1002/qj.2562, 2015.

Delworth, T. L., Zeng, F., Vecchi, G. A., Yang, X., Zhang, L., and Zhang, R.: The North Atlantic Oscillation as a driver of rapid climate change in the Northern Hemisphere, Nat. Geosci., 9, 509–513, https://doi.org/10.1038/ngeo2738, 2016.

Deser, C., Guo, R., and Lehner, F.: The relative contributions of tropical Pacific sea surface temperatures and atmospheric internal variability to the recent global warming hiatus, Geophys. Res. Lett., 44, 7945–7954, https://doi.org/10.1002/2017GL074273, 2017a.

Deser, C., Hurrell, J. W., and Phillips, A.S.: The role of the North Atlantic Oscillation in European climate projections, Clim. Dynam., 49, 3141–3157, https://doi.org/10.1007/s00382-016-3502-z, 2017b.

Deepshikha, S., Satheesh, S. K., and Srinivasan, J.: Dust aerosols over India and adjacent continents retrieved using METEOSAT infrared radiance Part II: quantification of wind dependence and estimation of radiative forcing, Annales Geophysicae, 24, 63–79, doi:10.5194/angeo-24-63-2006, 2006.

England, M. H., McGregor, S., Spence, P., Meehl, G. A., Timmermann, A., Cai, W., Gupta, A. S., McPhaden, M. J., Purich, A., and Santoso, A.: Recent intensification of wind-driven circulation in the Pacific and the on-going warming hiatus, Nat. Clim. Change, 4, 222–227, https://doi.org/10.1038/nclimate2106, 2014.

Feng, S. and Hu, Q.: How the North Atlantic Multidecadal Oscillation may have influenced the Indian summer monsoon during the past two millennia?, Geophys. Res. Lett., 35, L01707, doi:10.1029/2007GL032484, 2008.

Folland, C. K., Knight, J., Linderholm, H. W., Fereday, D., Ineson, S., and Hurrell, J. W.: The summer North Atlantic Oscillation: past, present, and future, J. Climate, 22, 1082–1103, 2009.

Gao, M., Sherman, P., Song, S., Yu, Y., Wu, Z., and McElroy, M. B.: Seasonal prediction of Indian wintertime aerosol pollution using the ocean memory effect, Sci. Adv., 5, eaav4157, https://doi.org/10.1126/sciadv.aav4157, 2019.

Gao, Y., Wang, H. J., and Chen, D.: Interdecadal variations of the South Asian summer monsoon circulation variability and the associated sea surface temperatures on interannual scales, Adv. Atmos. Sci., 34, 816–832, https://doi.org/10.1007/s00376-017-6246-8, 2017.

712 Gastineau, G. and Frankignoul, C.: Influence of the North Atlantic SST Variability on the Atmospheric
713 Circulation during the Twentieth Century, J. Climate, 28, 1396–1416, https://doi.org/10.1175/JCLI-D-14-
714 00424.1, 2015.

715 Ginoux, P., Prospero, J. M., Gill, T. E., Hsu, N. C., and Zhao, M.: Global-scale attribution of anthropogenic and
716 natural dust sources and their emission rates based on MODIS Deep Blue aerosol products, Rev. Geophys., 50,
717 RG3005, doi:10.1029/2012RG000388, 2012.

718 Goswami, B. N., Madhusoodanan, M., Neema, C., and Sengupta, D.: A physical mechanism for North Atlantic
719 SST influence on the Indian summer monsoon, Geophys. Res. Lett., 33, L02706,
720 https://doi.org/10.1029/2005GL024803, 2006.

721 Han, Z., Luo, F.F., and Wan, J.H.: The observational influence of the North Atlantic SST tripole on the early
722 spring atmospheric circulation, Geophys. Res. Lett., 43, 2998–3003, https://doi.org/10.1002/2016GL068099,
723 2016.

724 Hanf, F. S., and Annamalai, H.: Systematic Errors in South Asian Monsoon Precipitation: Process-Based
725 Diagnostics and Sensitivity to Entrainment in NCAR Models, J. Climate, 33, 2817–2840,
726 https://doi.org/10.1175/JCLI-D-18-0495.1, 2020.

727 Hirahara, S., Ishii, M., and Fukuda, Y.: Centennial-scale sea surface temperature analysis and its uncertainty, J.
728 Climate, 27, 57–75, https://doi.org/10.1175/JCLI-D-12-00837.1, 2014.

729 Hsu, N. C., Tsay, S. C., King, M. D., and Herman, J. R.: Aerosol Properties over Bright-Reflecting Source
730 Regions, IEEE T. Geosci. Remote, 42, 557–569, https://doi.org/10.1109/TGRS.2004.824067, 2004.

731 Hsu, N. C., Tsay, S.-C., King, M. D., and Herman, J. R.: Deep Blue retrievals of Asian aerosol properties during
732 ACE-Asia, IEEE T. Geosci. Remote Sens., 44, 3180–3195, https://doi.org/10.1109/TGRS.2006.879540, 2006.

733 Hu, S., and Fedorov, A.V.: The extreme El Niño of 2015–2016 and the end of global warming hiatus, Geophys.
734 Res. Lett., 44, 3816–3824, doi:10.1002/2017GL072908, 2017.

735 Huang B., Thorne, P. W., Banzon, V. F., Boyer, T., Chepurin, G., Lawrimore, J. H., Menne, M. J., Smith, T. M.,
736 Vose, R. S., and Zhang, H-M.: Extended Reconstructed Sea Surface Temperature, Version 5 (ERSSTv5):
737 Upgrades, Validations, and Intercomparisons, J. Climate, 30, 8179–8205, doi: 10.1175/JCLI-D-16-0836.1,
738 2017.

739 Huang, X., Zhou, T., Turner, A., Dai, A., Chen, X., Clark, R., and Zou, L.: The Recent Decline and Recovery of
740 Indian Summer Monsoon Rainfall: Relative Roles of External Forcing and Internal Variability, J. Climate, 33,
741 5035-5060, doi:10.1175/jcli-d-19-0833.1, 2020.

742 Huffman, G. J., Alder, R. F., Arkin, P., Chang, A., Ferraro, R., Gruber, A., Janowiak, J., McNab, A., Rudolf, B.,
743 and Schneider, U.: The Global Precipitation Climatology Project (GPCP) Combined Precipitation Dataset, B.
744 Am. Meteorol. Soc., 78, 5–20, https://doi.org/10.1175/1520-0477(1997)078<0005:TGPCPG>2.0.CO;2, 1997.

Hurrell, J. W.: Decadal trends in the North Atlantic oscillation: Regional temperatures and precipitation, Science, 269, 676–679, https://doi.org/10.1126/science.269.5224.676, 1995.

Hurrell, J. W., Hack, J. J., Shea, D., Caron, J. M., and Rosinski, J.: A New Sea Surface Temperature and Sea Ice Boundary Dataset for the Community Atmosphere Model, J. Climate, 21, 5145–5153, https://doi.org/10.1175/2008JCLI2292.1, 2008.

~~Hurrell, J. W., and Deser C.: North Atlantic climate variability: the role of the North Atlantic Oscillation, J. Marine Syst., 79(3), 231-244, https://doi.org/10.1016/j.jmarsys.2009.11.002, 2009.~~

Hurrell, J. W., and Deser C.: North Atlantic climate variability: the role of the North Atlantic Oscillation, J. Marine Syst., 78, 28-41, https://doi.org/10.1016/j.jmarsys.2008.11.026, 2009.

Iles, C., and Hegerl, G.: Role of the North Atlantic Oscillation in decadal temperature trends, Environ. Res. Lett., 12, 114010, https://doi.org/10.1088/1748-9326/aa9152, 2017.

Jin, Q., Wei, J., and Yang, Z.-L.: Positive response of Indian summer rainfall to Middle East dust, Geophys. Res. Lett., 41, 4068–4074, https://doi.org/10.1002/2014GL059980, 2014.

Jin, Q., Wei, J., Pu, B., Yang, Z. L., and Parajuli, S. P.: High summertime aerosol loadings over the Arabian Sea and their transport pathways, J. Geophys. Res.- Atmos., 123, 10568–10590, https://doi.org/10.1029/2018jd028588, 2018a.

Jin, Q., and Wang, C.: The greening of Northwest Indian subcontinent and reduction of dust abundance resulting from Indian summer monsoon revival, Sci Rep., 8, 4573, https://doi.org/10.1038/s41598-018-23055-5, 2018b.

Kalnay, E., Kanamitsu, M., Kistler, R., Collines, W., Deaven, D., Gandin, L., Iredell, M., Saha, S., White, G., Woollen, J., Zhu, Y., Leetmaa, A., Reynolds, R., Chelliah, M., Ebisuzaki, W., Higgins, W., Janowiak, J., Mo, K. C., Ropelewski, C., and Wang, J.: The NCEP/NCAR 40-year reanalysis project, B. Am. Meteorol. Soc., 77, 437–471, doi:10.1175/1520-0477(1996)077<0437:Tnyrp>2.0.Co;2, 1996.

Kim, M.-K., Lau, W. K. M., Kim, K.-M., Sang, J., Kim, Y.-H., and Lee, W.-S.: Amplification of ENSO effects on Indian summer monsoon by absorbing aerosols, Clim. Dynam., 46, 2657–2671, https://doi.org/10.1007/s00382-015-2722-y, 2016.

Kinter III, J., Miyakoda, K., and Yang, S.: Recent change in the connection from the Asian monsoon to ENSO, J. Climate, 15, 1203–1215, https://doi.org/10.1175/1520-0442(2002)015<1203:RCITCF>2.0.CO;2, 2002.

Kosaka, Y., and Xie, S. P.: Recent global-warming hiatus tied to equatorial Pacific surface cooling, Nature, 501, 403–407, doi:https://doi.org/10.1038/nature12534, 2013.

Kosaka, Y., and Xie , S. P.: The tropical Pacific as a key pacemaker of the variable rates of global warming, Nat. Geosci., 9, 669–673,doi:10.1038/ngeo2770, 2016.

Krishnamurthy, L., and Krishnamurthy, V.: Teleconnections of Indian monsoon rainfall with AMO and Atlantic tripole, Clim. Dynam., 46, 2269–2285, doi:https://doi.org/10.1007/s00382-015-2701-3, 2015.

Kucharski, F., Bracco, A., Yoo, J. H., and Molteni, F.: Low-frequency variability of the Indian monsoon – ENSO relation and the Tropical Atlantic: the "weakening" of the '80s and '90s, J. Climate, 20, 4255–4266, https://doi.org/10.1175/JCLI4254.1, 2007.

Kucharski, F., Bracco, A., Yoo, J. H., and Molteni, F.: Atlantic forced component of the Indian monsoon interannual variability, Geophys. Res. Lett., 35, L04706, doi:10.1029/2007GL033037, 2008.

Kumar, K. K., Rajagopalan, B., and Cane, K. A.: On the weakening relationship between the Indian Monsoon and ENSO, Science, 284, 2156–2159, https://doi.org/10.1126/science.284.5423.2156, 1999.

~~Kumar, K. K., Rajagopalan, B., Hoerling, M., Bates, G., Cane, M. A.: Unraveling the Mystery of Indian Monsoon Failure During El Ni˜no, Science, 314, 115–119, https://doi.org/10.1126/science.1131152, 2006.~~

Kumar, K. K., Rajagopalan, B., Hoerling, M., Bates, G., Cane, M. A.: Unraveling the mystery of Indian monsoon failure during El Niño, Science, 314, 115–119, https://doi.org/10.1126/science.1131152, 2006.

Lee, T. and McPhaden, M. J.: Increasing intensity of El Niño~~Ni˜no~~ in the central-equatorial Pacific, Geophys. Res. Lett., 37, L14603, https://doi.org/10.1029/2010GL044007, 2010.

Liu, W., Fedorov, A. V., Xie, S. P., and Hu, S.: Climate impacts of a weakened Atlantic Meridional Overturning Circulation in a warming climate, Sci. Adv., 6, eaaz4876, https://doi.org/10.1126/sciadv.aaz4876, 2020.

Mahowald, N. M., Muhs, D. R., Levis, S., Rasch, P. J., Yoshioka, M., Zender, C. S., and Luo, C.: Change in atmospheric mineral aerosols in response to climate: Last glacial period, preindustrial, modern, and doubled carbon dioxide climates, J. Geophys. Res.-Atmos., 111, D10202, https://doi.org/10.1029/2005JD006653, 2006.

Mariotti, A., Zeng, N., and Lau, K.-M.: Euro-Mediterranean rainfall and ENSO – a seasonally varying relationship, Geophys. Res.Lett., 29, 1621–1625, doi:10.1029/2001GL014248, 2002.

Marticorena, B., and Bergametti, G.: Modeling the atmospheric dust cycle.1. Design of a soil-derived emission scheme, J. Geophys. Res.--Atmos., 100, 16415–16430, 1995.

Mohtadi, M., Prange, M., Oppo, D.W., De Pol-Holz, R., Merkel, U., Zhang, X., Steinke, S., and Lückge, A.: North Atlantic forcing of tropical Indian Ocean climate, Nature, 509, 76–80, 2014.

Neale, R. B., Richter, J. H., Conley, A. J., Park, S., Lauritzen, P. H., and Gettleman, A.: Description of the NCAR Community Atmosphere Model (CAM 4.0), NCAR Tech. Note NCAR/TN-485+STR, 212 pp., www.cesm.ucar.edu/models/ccsm4.0/cam/docs/description/cam4_desc.pdf, 2010.

Notaro, M., Yu, Y., and Kalashnikova, O. V.: Regime shift in Arabian dust activity, triggered by persistent fertile crescent drought, J. Geophys. Res.--Atmos., 120, 10229–10249, https://doi.org/10.1002/2015JD023855, 2015.

Osborne, J. M., Collins, M., Screen, J. A., Thomson, S. I., and Dunstone, N.: The North Atlantic as a Driver of Summer Atmospheric Circulation, J. Climate, 33, 7335–7351, https://doi.org/10.1175/JCLI-D-19-0423.1, 2020.

Ossó, A., Sutton, R., Shaffrey, L., and Dong, B.: Observational evidence of European summer weather patterns predictable from spring, Proc. Natl. Acad. Sci. USA, 115, 59–63, https://doi.org/10.1073/pnas.1713146114, 2018.

Ossó, A., Sutton, R., Shaffrey, L., and Dong, B.: Development, Amplification, and Decay of Atlantic/European Summer Weather Patterns Linked to Spring North Atlantic Sea Surface Temperatures, J. Climate, 33, 5939–5951, https://doi.org/10.1175/JCLI-D-19-0613.1, 2020.

Pandey, S. K., Vinoj, V., Landu, K., and Babu, S. S.: Declining pre-monsoon dust loading over South Asia: Signature of a changing regional climate, Sci. Rep., 7, 16062, https://doi.org/10.1038/s41598-017-16338-w, 2017.

Pandithurai, G., Dipu, S., Dani, K. K., Tiwari, S., Bisht, D. S., Devara, P. C. S., and Pinker, R. T.: Aerosol radiative forcing during dust events over New Delhi, India, J. Geophys. Res.-Atmos., 113, D13209, doi:10.1029/2008JD009804, 2008.

Pourmand, A., Marcantonio, F., and Schulz, H.: Variations in productivity and eolian fluxes in the northeastern Arabian Sea during the past 110 ka, Earth Planet. Sci. Lett., 221, 39–54, doi:10.1016/S0012-821X(04)00109-8, 2004.

Pu, B. and Ginoux, P.: The impact of the Pacific Decadal Oscillation on springtime dust activity in Syria, Atmos. Chem.Phys., 16, 13431–13448, https://doi.org/10.5194/acp-16-13431-2016, 2016.

Pu, B. and Ginoux, P.: How reliable are CMIP5 models in simulating dust optical depth?, Atmos. Chem. Phys., 18, 12491–12510, https://doi.org/10.5194/acp-18-12491-2018, 2018.

Rajeevan, M., and Sridhar, L.: Inter-annual relationship between Atlantic sea surface temperature anomalies and Indian summer monsoon, Geophys. Res. Lett., 35, L21704, doi:10.1029/2008GL036025, 2008.

Ramanathan, V., Chung, C., Kim, D., Bettge, T., Buja, L., Kiehl, J. T., Washington, W. M., Fu, Q., Sikka, D. R., and Wild, M.: Atmospheric brown clouds: Impacts on South Asian climate and hydrological cycle, P. Natl. Acad. Sci. USA, 102, 5326–5333, https://doi.org/10.1073/pnas.0500656102, 2005.

Rasmusson, E. M., and Carpenter, T.H.: The relationship between eastern equatorial Pacific sea surface temperatures and rainfall over India and Sri Lanka, Mon, Weather Rev., 111, 517–528, 1983.

Rayner, N. A., Parker, D. E., Horton, E. B., Folland, C. K., Alexander, L. V., Rowell, D. P., Kent, E. C., and Kaplan, A.: Global analyses of sea surface temperature, sea ice, and night marine air temperature since the late nineteenth century, J. Geophys. Res.-Atmos., 108, 4407, https://doi.org/10.1029/2002JD002670, 2003.

Reynolds, R. W., Rayner, N. A., Smith, T. M., Stokes, D. C., and Wang, W.: An improved in situ and satellite SST analysis for climate, J. Climate, 15, 1609–1625, https://doi.org/10.1175/1520-0442(2002)015<1609:AIISAS>2.0.CO;2, 2002.

Rodwell, M. J., Rowell, D. P., and Folland, C. K.: Oceanic forcing of the wintertime North Atlantic Oscillation and European climate, Nature, 398, 320–323, https://doi.org/10.1038/18648, 1999.

Sabeerali, C. T., Ajayamohan, R. S., Bangalath, H. K., and Chen, N.: Atlantic Zonal Mode: an emerging source of Indian summer monsoon variability in a warming world, Geophys. Res. Lett., 46, 4460–4464, https://doi.org/10.1029/2019GL082379, 2019.

Safaierad, R., Mohtadi, M., Zolitschka, B., Yokoyama, Y., Vogt, C., Schefuß, E.: Elevated dust depositions in West Asia linked to ocean–atmosphere shifts during North Atlantic cold events, Proc. Natl. Acad. Sci.USA,117 (31) 18272-18277, doi: 10.1073/pnas.2004071117, 2020.

Sanap, S. D., Ayantika, D. C., Pandithurai, G., and Niranjan, K.: Assessment of the aerosol distribution over Indian subcontinent in CMIP5 models, Atmos. Environ., 87, 123–137, https://doi.org/10.1016/j.atmosenv.2014.01.017, 2014.

Satheesh, S. K., and Ramanathan, V.: Large differences in tropical aerosol forcing at the top of the atmosphere and Earth's surface, Nature, 405**,** 60–63, 2000.

Sikka, D. R.: Some aspects of the large scale fluctuations of summer monsoon rainfall over India in relation to fluctuations in the planetary and regional scale circulation parameters, Proc. Ind. Acad. Sci. (Earth & Planet. Sci.) , 89, 179–195, 1980.

Solmon, F., Nair, V. S., and Mallet, M.: Increasing Arabian dust activity and the Indian summer monsoon, Atmos. Chem. Phys.,15, 8051–8064, doi:10.5194/acp-15-8051-2015, 2015.

Sperber, K. R., Annamalai, H., Kang, I.-S., Kitoh, A., Moise, A., Turner, A., Wang, B., and Zhou, T.: The Asian summer monsoon: an intercomparison of CMIP5 vs. CMIP3 simulations of the late 20th century, Clim. Dynam., 41, 2711–2744, https://doi.org/10.1007/s00382-012-1607-6, 2013.

Srivastava, A. K., Rajeevan, M., and Kulkarni, R.: Teleconnection of OLR and SST anomalies over Atlantic Ocean with Indian summer monsoon, Geophys. Res. Lett., 29(8), 1284, doi:10.1029/2001GL013837, 2002.

Srivastava, G., Chakraborty, A., and Nanjundiah, R.S.: Multidecadal see-saw of the impact of ENSO on Indian and West African summer monsoon rainfall, Clim Dynam., 52**,** 6633–6649, doi:10.1007/s00382-018-4535-2, 2019.

Stocker, T. F., Qin, D., Plattner, G.-K., Tignor, M., Allen, S. K., Boschung, J., Nauels, A., Xia, Y., Bex, V., and Midgley, P. M.: Climate Change 2013: The Physical Science Basis. Contribution of Working Group I to the Fifth Assessment Report of the Inter-governmental Panel on Climate Change, Cambridge University Press, 2013.

Sun, J. Q., Wang, H. J., and Yuan, W.: Role of the tropical Atlantic sea surface temperature in the decadal change of the summer North Atlantic Oscillation, J. Geophys. Res.-Atmos., 114, D20110, doi:10.1029/2009JD012395, 2009.

Trenberth, K. E. and Fasullo, J. T.: An apparent hiatus in global warming?, Earth's Future, 1, 19–32, https://doi.org/10.1002/2013EF000165, 2013.

Trenberth, K. E., Fasullo, J. T., Branstator, G., and Phillips, A. S.: Seasonal aspects of the recent pause in surface warming, Nat. Clim. Change, 4, 911–916, doi:10.1038/nclimate2341, 2014.

Thompson, L. G., Yao, T., Mosley-Thompson, E., Davis, M. E., Henderson, K. A., and Lin, P. N.: A high-resolution millennial record of the South Asian Monsoon from Himalayan ice cores, Science, 289, 1916–1919, 2000.

Vinoj, V., Rasch, P., Wang, H., Yoon, J., Ma, P., Landu, K., and Singh, B.: Short-term modulation of Indian summer monsoon rainfall by West Asian dust, Nat. Geosci., 7, 308–313, https://doi.org/10.1038/ngeo2107, 2014.

Visbeck, M., Cullen, H., Krahmann, G., and Naik, N.: An ocean model's response to North Atlantic Oscillation-like wind forcing, Geophys. Res. Lett., 25, 4521–4524, 1998.

Visbeck, M. H., Hurrell, J. W., Polvani, L., and Cullen, H. M.: The North Atlantic Oscillation: past, present and future, P. Natl. Acad. Sci. USA, 98, 12876–12877, 2001.

Walker, A. L., Liu, M., Miller, S. D., Richardson, K. A., and Westphal, D. L.: Development of a dust source database for mesoscale forecasting in southwest Asia, J. Geophys. Res.-Atmos., 114, D18207, doi:10.1029/2008JD011541, 2009.

Wang, B., Xiang, B., Li, J., Webster, P. J., Rajeevan, M. N., Liu, J., and Ha, K.-J.: Rethinking Indian monsoon rainfall prediction in the context of recent global warming, Nat. Commun., 6, 7154, https://doi.org/10.1038/ncomms8154, 2015.

Wulff, C. O., Greatbatch, R. J., Domeisen, D. I. V., Gollan, G., and Hansen, F.: Tropical forcing of the summer east Atlantic pattern, Geophys. Res. Lett., 44, 11 166–11 173, https://doi.org/10.1002/2017GL075493, 2017.

Xie, S.-P., and Kosaka, Y.: What caused the global surface warming hiatus of 1998–2013? Curr. Climate Change Rep., 3, 128–140, https://doi.org/10.1007/s40641-017-0063-0, 2017.

Yeh, S.-W., Kug, J.-S., Dewitte, B., Kwon, M.-H., Kirtman, B.P., and Jin, F.-F.: El Niño in a changing climate, Nature, 461, 511–514, 2009.

Yu, Y., Notaro, M., Liu, Z., Wang, F., Alkolibi, F., Fadda, E., and Bakhrjy, F.: Climatic controls on the interannual to decadal variability in Saudi Arabian dust activity: toward the development of a seasonal dust prediction model, J. Geophys. Res.- Atmos., 120, 1739–1758, https://doi.org/10.1002/2014JD022611, 2015.

Zender, C. S., Bian, H., and Newman, D.: Mineral Dust Entrainment and Deposition (DEAD) model: Description and 1990s dust climatology, J. Geophys. Res.-Atmos., 108, 4416, https://doi.org/10.1029/2002JD002775, 2003a.

Zender, C. S., Newman, D., and Torres, O.: Spatial heterogeneity in aeolian erodibility: uniform, topographic, geomorphic and hydrologic hypotheses, J. Geophys. Res.-Atmos., 108, 4543, doi:10.1029/2002JD003039, 2003b.

Zhang, R. and Delworth, T. L.: Impact of Atlantic multidecadal oscillations on India/Sahel rainfall and Atlantic hurricanes, Geophys. Res. Lett., 33, L17712, doi:10.1029/2006GL026267, 2006.

Zhu, A., Ramanathan, V., Li, F., and Kim, D.: Dust plumes over the Pacific, Indian, and Atlantic oceans: climatology and radiative impact, J. Geophys. Res.-Atmos., 112, D16208, doi:10.1029/2007JD008427, 2007.